

Denoising Data with Measurement Error Using a Reproducing Kernel-based Diffusion Model

Mingyang Yi^a, Marcos Matabuena^b, and Ruoyu Wang^{b*}

^aSchool of Information, Renmin University of China, Beijing, P.R. China

^bDepartment of Biostatistics, Harvard T.H. Chan School of Public Health, Boston, MA, USA

Abstract

The ongoing technological revolution in measurement systems enables the acquisition of high-resolution samples in fields such as engineering, biology, and medicine. However, these observations are often subject to errors from measurement devices. Motivated by this challenge, we propose a denoising framework that employs diffusion models to generate denoised data whose distribution closely approximates the unobservable, error-free data, thereby permitting standard data analysis based on the denoised data. The key element of our framework is a novel Reproducing Kernel Hilbert Space-based method that trains the diffusion model with only error-contaminated data, admits a closed-form solution, and achieves a fast convergence rate in terms of estimation error. Furthermore, we verify the effectiveness of our method by deriving an upper bound on the Kullback–Leibler divergence between the distributions of the generated denoised data and the error-free data. A series of conducted simulations also verify the promising empirical performance of the proposed method compared to other state-of-the-art methods. To further illustrate the potential of this denoising framework in a real-world application, we apply it in a digital health context, showing how measurement error in continuous glucose monitors can influence conclusions drawn from a clinical trial on diabetes Mellitus disease.

Keywords: Digital health, Error-contaminated data, Generative model, Machine learning, Score matching.

* Corresponding author. Email: ruoyuwang@hsph.harvard.edu

1 Introduction

In the current artificial intelligence (AI) era, machine learning-based predictions have become central to applied data analysis across various fields. In parallel, the ongoing technological revolution in measurement systems now enables the acquisition of extremely high-resolution data, generating large-scale samples across diverse scientific domains—such as engineering, biology, and medicine—with the potential for groundbreaking insights. However, these measurements are frequently subject to significant device errors, which can compromise the discoveries and predictions (Carroll et al., 2006). Collecting error-free measurements remains a major challenge in many modern research problems, including epidemiology (Loken and Gelman, 2017), clinical trials (Lachin, 2004), agriculture (Desiere and Jolliffe, 2018), econometrics (Thompson and Carter, 2007), computer vision (Brodley and Friedl, 1999; Xiao et al., 2015), and natural language processing (Garg et al., 2021; Havrilla and Iyer, 2024). However, state-of-the-art machine learning methods often are not designed to handle measurement-related errors in observed data (Li et al., 2021; Song et al., 2022a). Such oversight can critically impact decision-making processes; for instance, in medicine, an inaccurate diagnosis or patient reclassification can have serious consequences from the clinical, social, and economic points of view.

Methods that account for potential measurement errors and produce valid statistical inferences have predominantly arisen in statistical science, often motivated by specific applications, such as in medicine, and with a historical focus in signal processing. Examples of these methods include the observed likelihood approach (Zucker, 2005), the conditional score method (Stefanski and Carroll, 1987), the corrected estimating equation method (Nakamura, 1990; Wang and Sullivan Pepe, 2000; Wang et al., 2012), and simulation-based exploration techniques (Carroll et al., 1996). These classical methods address the measurement error by constructing asymptotically unbiased estimators from error-contaminated data. However, deriving such estimators is nontrivial, often model-specific, and may require expertise beyond that of the typical investigator. In addition, all the above methods are based on asymptotic theories for classic estimators such as M -estimators.

It is not straightforward to extend the above methods to accommodate common machine learning methods whose asymptotic properties can be complicated and understudied. Another line of research considers the deconvolution problem, which aims to recover the distribution of error-free data from error-contaminated observations. Most existing deconvolution methods focus on the univariate case (Zhang, 1990; Fan, 1991; Cordy and Thomas, 1997; Delaigle and Hall, 2008; Meister and Neumann, 2010; Lounici and Nickl, 2011; Guan, 2021; Belomestny and Goldenshluger, 2021). A handful of approaches address the multivariate setting, typically via normal mixture models (Bovy et al., 2011; Sarkar et al., 2018) or kernel smoothing (Masry, 1993; Lepski and Willer, 2019). However, normal mixture models can be highly sensitive to misspecification, whereas kernel smoothing methods tend to converge slowly (polynomial of $1/\log n$, n is the sample size) in deconvolution problems with normal error (Fan, 1991) and suffer from the curse of dimensionality in multivariate scenarios (Masry, 1993). Consequently, these limitations hinder the application of classical non-parametric statistical methods to more complex models across diverse research areas and new emerging scientific problems. For example, modern data collection practices have enabled high-dimensional data, such as medical imaging, and other emerging data structures (Loh and Wainwright, 2012; Jiang et al., 2023). These developments pose additional challenges for classical methods. As a result, researchers are increasingly turning to machine learning approaches—such as neural networks (LeCun et al., 2015) and kernel-based statistical learning in reproducing kernel Hilbert spaces (RKHS) (De Vito et al., 2005) which can empirically outperform classical nonparametric techniques such as kernel smoothing techniques in large-dimensional settings.

In the emerging field of machine learning, learning with error-contaminated data has received significant attention, especially for deep learning models (LeCun et al., 2015). In contrast to statistics, which focuses on statistical inference based on error-contaminated data, researchers in the AI community are primarily concerned with training models (usually neural networks) on error-contaminated data, aiming for accurate predictions based solely on error-free data. Methods in this field often focus on constructing “robust loss” functions, which enhance model robustness

when trained on error-contaminated data (Song et al., 2022a; Yi et al., 2021; Wang et al., 2022; Yi et al., 2023b). However, these methods mainly apply to scenarios with low-level errors and are restricted to classification problems, often requiring high computational costs.

The combination of statistical inferential thinking with machine learning offers the opportunity to develop novel methods for tackling the measurement error problem. In this paper, we explore this interface through a powerful generative model, the diffusion model originated from machine learning (Hyvärinen and Dayan, 2005; Vincent, 2011), which has been shown to outperform classical generative models in multiple practical applications (Song et al., 2022b; Ho et al., 2020; Rombach et al., 2022; Song et al., 2021). Specifically, we focus on the case with a normal measurement error, which is commonly adopted in the measurement error literature (Yi, 2017). In contrast to the aforementioned standard methods, we directly generate denoised data whose distribution is close to the error-free ones, so that any downstream analysis can be conducted based on the denoised data. The idea of a diffusion model is to transfer a normal noise into a target distribution by gradually removing the noise in it, through a diffusion process. In the diffusion model, the generation process moves along the trajectory of a stochastic differential equation (SDE), roughly speaking, “noise” \rightarrow “error-contaminated data” \rightarrow “error-free data”. Thus, it is a natural fit for transforming “error-contaminated data” to “error-free data” in measurement error problems. However, applying the diffusion technique is not straightforward in the measurement error context. Specifically, the diffusion model requires estimating the “score function” (Hyvärinen and Dayan, 2005) of the intermediate error-contaminated data (Song et al., 2022b; Ho et al., 2020), which is the drift term (Oksendal, 2013) in the SDE of the diffusion model. Unfortunately, the intermediate error-contaminated data are unobserved in measurement error problems in practice. To overcome this challenge, we propose a complex-value score-matching loss function that can be adopted to estimate the score function of the intermediate error-contaminated data based solely on the observed error-contaminated data. We propose a novel RKHS-based score-matching method to address the implementation challenges associated with complex numbers. When implemented with

a Gaussian kernel, all the complex numbers involved in the complex-value score-matching loss can be integrated, enabling the estimated score function to be obtained without directly operating on complex numbers. Furthermore, the resulting score estimator is available in closed form, offering significant computational convenience.

When using the denoised data to conduct downstream analysis, the correctness of the downstream analysis depends on the gap between the distributions of the denoised data and the error-free ones. We characterize such a gap by the Kullback–Leibler (KL) divergence between the two distributions under proper regularity conditions. With n observed data, we prove that the error in terms of KL divergence is of order $\mathcal{O}_P((\mathcal{B}_K/n)^{-1/2})$ which implies a total variation distance bound of order $\mathcal{O}_P((\mathcal{B}_K/n)^{-1/4})$, where \mathcal{B}_K is a constant defined in Assumption 1 that may depend on the dimension d of the observation and can scale with the dimension of data d in the order of $\mathcal{O}(c^d)$ for some $c > 1$. Numerical results in simulation studies show the promising empirical performance of the proposed method. An application to the digital heal trial data collected by the Juvenile Diabetes Research Foundation (JDRF) Continuous Glucose Monitoring (CGM) Study Group (Tamborlane et al., 2008; JDRF CGM Study Group, 2009) illustrates the practical value in clinical applications.

1.1 Practical Motivation: Quantifying the Impact of Measurement Error in Medical Devices for Digital Health Trials

AI-based algorithms are enabling a new era in clinical systems, driven by the rapid development of wearable and implantable technology in digital health. Modern medical devices have the potential to transform healthcare by recording physiological variables—such as glucose levels, heart rate, and step cadence—over prolonged periods. With these technologies, clinicians can improve medical diagnostics and tailor treatments in a more personalized manner across diverse clinical situations.

Despite these technological advances and novel therapeutic opportunities, new statistical and machine learning methods are required to account for the peculiarities of measurement technologies and emerging data structures (Zhang et al., 2024). For illustration, we consider the clinical trial

data collected by the JDRF CGM Study Group to evaluate clinical interventions through CGM. In this context, understanding and quantifying the impact of CGM measurement error is crucial for clinical-decision makings such as the evaluation of the effectiveness of interventions and new drugs. The proposed method can be a valuable tool in digital health clinical trials as well as for the regulatory medical agencies to define new safety validation criteria.

1.2 Paper Contributions

The contributions of this paper are outlined below:

1. **Flexible and Scalable Diffusion-Based Method:** We propose a flexible and scalable diffusion-based denoising framework that synthetic error-free data. Then, statistical and machine learning methods can be applied to them for any downstream tasks, e.g., predictive or unsupervised learning tasks. Our method does not require the density of the error-free data to follow a parametric form and is applicable in large-scale multivariate datasets.
2. **Novel Non-parametric RKHS Framework:** To achieve tractable and efficient estimation with favorable convergence properties, we propose a non-parametric diffusion framework in an RKHS setting with a Gaussian kernel, based on a complex score-matching loss function. This approach enables us to estimate the score function of intermediate error-contaminated data using only the observed, error-contaminated data.
3. **Provable Convergence Rate:** Under proper regularity conditions, we prove that our diffusion-based denoised data distribution approximates the error-free ones with the KL divergence between them of order $\mathcal{O}(1/\sqrt{\mathcal{B}_K/n})$, which matches the standard results in the existing literature of diffusion-based methods in the error-free case (Chen et al., 2022; Lee et al., 2022). Notably, the KL convergence result indicates a faster rate than the classical kernel smoothing-based deconvolution distribution estimator (Fan, 1991). Such an acceleration comes from additional smoothness conditions imposed on the score function, which are not introduced in traditional deconvolution methods.

4. **Application to Real Data in Digital Health:** We demonstrate the flexibility and applicability of the proposed framework through a real-world clinical problem in the digital health domain, specifically examining the impact of measurement error on decision-making for CGM. Our sensitivity analysis provides a novel opportunity to reevaluate diabetes clinical trials by incorporating the measurement error of continuous glucose monitors and drawing valid conclusions about the effects of new interventions and drugs.

1.3 Outline

The rest of this paper is organized as follows. Section 2 provides some preliminaries. In Section 3, we propose the RKHS-based diffusion model that can generate error-free data using error-contaminated data. Our theoretical analysis is mainly in Section 4, where we characterize the sampling error measured by KL divergence between the generated denoised data and the error-free ones. Sections 5 and 6 present some simulation results and a real world application of our proposed method. Section 7 is the discussion of this paper. Supplementary Material contains all the proofs, additional backgrounds, related work, assumptions, and numerical experiments.

2 Notations and Preliminaries to Diffusion Model

Notations. We use \mathbb{E} to denote expectation and use a subscript if the expectation is taken w.r.t. some variables if necessary. We omit the subscript if the expectation is taken over all random variables. Constants related to the dimension d of the data and the data-generating process may be hidden in the order notations \mathcal{O} and \mathcal{O}_P , while we try to preserve important constants that can be relevant to the finite-sample performance. For a random vector \mathbf{X} , $P_{\mathbf{X}}$ is its probability distribution. Let $\mathcal{H}_{\mathcal{K}}$ denote an RKHS induced by a positive semi-definite kernel $\mathcal{K}(\cdot, \cdot)$ defined on the product space \mathbb{C}^d of the complex plane \mathbb{C} . The kernel is a Gaussian kernel throughout this paper. For any $f \in \mathcal{H}_{\mathcal{K}}$ and $\mathbf{x} \in \mathbb{C}^d$, the kernel satisfies the reproducing property $\langle \mathcal{K}(\cdot, \mathbf{x}), f \rangle_{\mathcal{H}_{\mathcal{K}}} = f(\mathbf{x})$ where $\langle \cdot, \cdot \rangle_{\mathcal{H}_{\mathcal{K}}}$ is the inner product in $\mathcal{H}_{\mathcal{K}}$. Let $\mathcal{H}_{\mathcal{K}}^d = \mathcal{H}_{\mathcal{K}} \times \cdots \times \mathcal{H}_{\mathcal{K}}$ be a d -dimensional RKHS with inner product defined as the summation of componentwise inner products.

The goal is to sample denoised data from the target distribution with only error-contaminated data observed. Let $\{\mathbf{X}_0^{(i)}\}_{i=1}^n$ be a random sample from the target distribution $P_{\mathbf{X}_0}$ of the d -dimensional error-free data. The observed error-contaminated dataset is $\{\mathbf{X}_1^{(i)}\}_{i=1}^n$, with $\mathbf{X}_1^{(i)} = \mathbf{X}_0^{(i)} + \epsilon^{(i)}$ for $i = 1, \dots, n$, where $\mathbf{X}_0^{(i)} \perp \epsilon^{(i)}$. We assume $\{\epsilon^{(i)}\}_{i=1}^n$ are all random errors that follow $\mathcal{N}(\mathbf{0}, \Sigma)$. To focus on the main idea, we consider the case where the measurement error is normal with zero mean and known variance in this paper. Σ can be estimated using observed data if a validation sample or replicated measurements are available (Yi, 2017).

Define the level-controlled error-contaminated data $\mathbf{X}_t = \mathbf{X}_0 + \Sigma^{\frac{1}{2}} \mathbf{W}_t$, and denote its distribution and density by $P_{\mathbf{X}_t}$ and p_t , respectively, where $\mathbf{W}_t \in \mathbb{R}^d$ is the standard Brownian motion. \mathbf{X}_t may not have actual meaning in the real world and we do not require that there is some Brownian motion which connects the error-free and error-contaminated observation, The level-controlled error-contaminated data is just of conceptual importance to understand the diffusion model.

Preliminaries to Diffusion Model. The diffusion model was firstly proposed in (Sohl-Dickstein et al., 2015) as a technique of data generation in the AI community. Theoretically, the technique is an application of multi-step variational auto-encoder (Kingma and Welling, 2013) and Langevin dynamics sampling (Hyvärinen and Dayan, 2005; Vincent, 2011; Chewi, 2023). Recently, with the development of deep learning, Ho et al. (2020) and Song et al. (2020b) rebuild this technique, and successfully apply it to high-resolution image generation tasks. In this paper, the framework of diffusion model is built upon the continuous-time SDE (Oksendal, 2013) as in (Song et al., 2022b). That says, for diffusion process $\mathbf{X}_t \in \mathbb{R}^d$ ($t \in [0, 1]$) satisfies

$$d\mathbf{X}_t = \mathbf{f}(\mathbf{X}_t, t)dt + \mathbf{g}(t)d\mathbf{W}_t, \quad (1)$$

started from $\mathbf{X}_0 \sim P_{\mathbf{X}_0}$ with known $\mathbf{f} \in \mathbb{R}^d$, $\mathbf{g} \in \mathbb{R}^{d \times d}$, and standard Brownian motion \mathbf{W}_t . Under proper regularity conditions (Anderson, 1982), the following reverse SDE $\widetilde{\mathbf{X}}_t$

$$d\widetilde{\mathbf{X}}_t = - \left(\mathbf{f}(\widetilde{\mathbf{X}}_t, t) - \mathbf{g}(t)\mathbf{g}(t)^\top \nabla \log p_{1-t}(\widetilde{\mathbf{X}}_t) \right) dt + \mathbf{g}(t)d\mathbf{W}_t, \quad (2)$$

starting from $\widetilde{\mathbf{X}}_0 \sim P_{\mathbf{X}_1}$ satisfies that $P_{\widetilde{\mathbf{X}}_t} = P_{\mathbf{X}_{1-t}}$ for any $t \in [0, 1]$. The goal of diffusion model is to generate data from $P_{\mathbf{X}_0}$ given observations $\{\mathbf{X}_0^{(i)}\}_{i=1}^n$ from it. By properly choosing \mathbf{f} and \mathbf{g} in (1), the terminal distribution $P_{\mathbf{X}_1}$ is usually easy to sample from e.g., normal in most cases (Song et al., 2020b; Liu et al., 2022). Then, starting from easily sampled $\widetilde{\mathbf{X}}_0 \sim P_{\mathbf{X}_1}$, solving (2) can produce the observation $\widetilde{\mathbf{X}}_1$ which follow the target distribution $P_{\mathbf{X}_0}$. To do so, one need to estimate the “score function” $\nabla \log p_t$ of \mathbf{X}_t by minimizing the following score-matching objective

$$\min_{\boldsymbol{\theta}_t} \left\{ \mathbb{E} \left[\|\mathbf{s}_t(\mathbf{X}_t; \boldsymbol{\theta}_t) - \nabla \log p_t(\mathbf{X}_t)\|^2 \right] \right\}; \quad t \in [0, 1],$$

where $\mathbf{s}_t(\cdot; \boldsymbol{\theta}_t)$ is the specified model for the score function. The above objective function is infeasible because $\nabla \log p_t(\mathbf{x})$ is unknown. To address this, Hyvärinen and Dayan (2005) and Vincent (2011) propose the following feasible equivalent objective function

$$\min_{\boldsymbol{\theta}_t} \left\{ \mathbb{E} \left[\|\mathbf{s}_t(\mathbf{X}_t; \boldsymbol{\theta}_t)\|^2 \right] + 2\text{tr} \left\{ \mathbb{E} [\nabla \mathbf{s}_t(\mathbf{X}_t; \boldsymbol{\theta}_t)] \right\} \right\}; \quad t \in [0, 1]. \quad (3)$$

In the data generation task, observations from $P_{\mathbf{X}_t}$ can be obtained by implementing the SDE (1) starting from $\{\mathbf{X}_0^{(i)}\}_{i=1}^n$. Unfortunately, this is not possible for the measurement error problem studied in this paper, because the error-contaminated data \mathbf{X}_1 rather than the error-free \mathbf{X}_0 from the target distribution $P_{\mathbf{X}_0}$ is observed. We will give our solution to this problem later in Section 3.

3 The Estimation and Denoising Procedure

We propose to leverage the diffusion model (Song et al., 2020b; Ho et al., 2020) to generate denoised data that closely mirrors the distribution of error-free data. The diffusion model has garnered acclaim owing to its significant effectiveness in a vast array of tasks spanning multiple research domains, especially in generative AI. As mentioned in Section 1, the idea of leveraging the diffusion model to generate approximately error-free data is straightforward, as mentioned in Section 1. That says, implementing the reverse SDE (2) started from observed error-contaminated data $\{\mathbf{X}_1^{(i)}\}_{i=1}^n$. To do so, we should estimate the “score function” (Vincent, 2011) by solving problem (3). Unfortunately, as discussed in Section 1, solving (3) requires data from $P_{\mathbf{X}_t}$ which are unobserved in practice. In this section, we will present our solution to this problem.

3.1 Estimating Score Function

Note that the constructed level-controlled error-contaminated data $\mathbf{X}_t = \mathbf{X}_0 + \Sigma \mathbf{W}_t$ satisfies

$$d\mathbf{X}_t = \Sigma^{\frac{1}{2}} d\mathbf{W}_t, \quad t \in [0, 1], \quad (4)$$

which is a special case for SDE (1) with $\mathbf{f} = \mathbf{0}$ and $\mathbf{g} = \Sigma$. As discussed in Section 1, under proper regularity conditions (Supplementary Material B), $\widetilde{\mathbf{X}}_t$ generated from the following *reverse SDE*

$$d\widetilde{\mathbf{X}}_t = \Sigma \nabla \log p_{1-t}(\widetilde{\mathbf{X}}_t) dt + \Sigma^{\frac{1}{2}} d\mathbf{W}_t, \quad (5)$$

has the same distribution as \mathbf{X}_{1-t} in (4) for each t . Thus, we can get $\mathbf{X}_0 = \widetilde{\mathbf{X}}_1$ by implementing the reverse SDE (5) from the contaminated observation $\widetilde{\mathbf{X}}_0 = \mathbf{X}_1$. Please see the Proposition 3 in Supplementary Material C or (Anderson, 1982).for more details.

To implement the reverse SDE (5) in practice, we should estimate the score-function $\nabla \log p_t(\cdot)$ for each t . However, the standard objective (3) can not be estimated since we do not have data from $P_{\mathbf{X}_t}$. To resolve this, we resort to the following useful lemma from Stefanski and Cook (1995). With this, we show that target (3) can be properly estimated, even without samples from $P_{\mathbf{X}_t}$. To simplify the presentation, we always assume the expectation and the series summation are exchangeable for the Taylor series of an analytic function throughout the paper.

Lemma 1. *Let ξ_1 and ξ_2 be mean zero independent and identically distributed normal vectors. For any analytic function $f(\cdot)$ on \mathbb{C}^d , it holds that $\mathbb{E}_{\xi_1, \xi_2}[f(\mathbf{x} + \xi_1 + i\xi_2)] = f(\mathbf{x})$, where $i = \sqrt{-1}$ is the imaginary unit.*

To get some intuitions for this Lemma, we consider the univariate case where ξ_1 and ξ_2 are standard normal variables. Then, for any positive integer r , $\mathbb{E}[(\xi_1 + i\xi_2)^r] = 0$ and hence $\mathbb{E}[(x + \xi_1 + i\xi_2)^r] = x^r$ according to the binomial theorem and straightforward calculation. This suggests the Lemma 1 holds for all polynomials. The generalization to analytic functions is straightforward under regularity conditions since analytic functions can be expressed as Taylor series. The following corollary based on Lemma 1 paves the way to estimate the score of \mathbf{X}_t solely based on \mathbf{X}_1 .

Corollary 1. Let $\boldsymbol{\xi} \sim \mathcal{N}(\mathbf{0}, \boldsymbol{\Sigma})$ be a random vector independent of \mathbf{X}_0 and $\boldsymbol{\epsilon}$. If $\mathbf{s}_t(\mathbf{X}_t; \boldsymbol{\theta}_t)$ and $\nabla \mathbf{s}_t(\mathbf{X}_t; \boldsymbol{\theta}_t)$ are both analytic, then we have

$$\begin{aligned} & \mathbb{E}_{\mathbf{X}_t} \left[\|\mathbf{s}_t(\mathbf{X}_t; \boldsymbol{\theta}_t)\|^2 \right] + 2\text{tr} \{ \mathbb{E}_{\mathbf{X}_t} [\nabla \mathbf{s}_t(\mathbf{X}_t; \boldsymbol{\theta}_t)] \} = \\ & \mathbb{E}_{\mathbf{X}_1, \boldsymbol{\xi}} \left[\|\mathbf{s}_t(\mathbf{X}_1 + i\sqrt{1-t}\boldsymbol{\xi}; \boldsymbol{\theta}_t)\|^2 \right] + 2\text{tr} \{ \mathbb{E}_{\mathbf{X}_1, \boldsymbol{\xi}} [\nabla \mathbf{s}_t(\mathbf{X}_1 + i\sqrt{1-t}\boldsymbol{\xi}; \boldsymbol{\theta}_t)] \}, \end{aligned} \quad (6)$$

where $i = \sqrt{-1}$ is the imaginary unit.

Note that here $\|z\|^2$ is $\mathbf{z}^\top \mathbf{z}$ for any $\mathbf{z} \in \mathbb{C}^d$ instead of its norm. We adopt this convention because $\mathbf{z}^\top \mathbf{z}$ is analytic while the norm is not. The proof of this corollary is in Supplementary Material D.1. According to Corollary 1, we can directly estimate the objective (3) by

$$\mathbb{E}_{\mathbf{X}_1, \boldsymbol{\xi}} \left[\|\mathbf{s}_t(\mathbf{X}_1 + i\sqrt{1-t}\boldsymbol{\xi}; \boldsymbol{\theta}_t)\|^2 \right] + 2\text{tr} \{ \mathbb{E}_{\mathbf{X}_1, \boldsymbol{\xi}} [\nabla \mathbf{s}_t(\mathbf{X}_1 + i\sqrt{1-t}\boldsymbol{\xi}; \boldsymbol{\theta}_t)] \}, \quad (7)$$

without any observations from $P_{\mathbf{X}_t}$. Ideally, with the new objective (7) proposed, in (2), starting from $\mathbf{X}_1^{(i)}$, and substituting the ground-truth score function $\nabla \log p_t(\cdot)$ with its approximation $\mathbf{s}_t(\cdot; \boldsymbol{\theta}_t)$. We can generate desired denoised data. Next, let us check this process in details.

3.2 Kernel-based Score Function

Note that in (7): (i) the model $\mathbf{s}_t(\cdot; \boldsymbol{\theta}_t)$ is supposed to be analytic in \mathbb{C}^d , which can be violated by many commonly-used nonparametric basis functions such as the B-spline; (ii) the objective function involves the Jacobian of the model and integrals with respect to some complex normal vector, which may cause a lot computational burden and numerical instability when minimizing it. To address these issues, one should specify a model $\mathbf{s}_t(\cdot; \boldsymbol{\theta}_t)$ which is (i) analytic; (ii) can approximate nonparametric smooth functions; (iii) permits the explicit computation of the expectation with respect to $i\sqrt{1-t}\boldsymbol{\xi}$. These properties ensure the nonparametric validity of the score estimator and the computational efficiency of the evaluation of the loss function at the sample level. To this end, we develop a method that satisfies all the above requirements based on the d -dimensional RKHS (please refer to Supplementary Material I for more details) $\mathcal{H}_{\mathcal{K}}^d$ associated with the positive semi-definite Gaussian kernel

$$\mathcal{K}(\mathbf{x}_1, \mathbf{x}_2) = \exp \left\{ -(\mathbf{x}_1 - \bar{\mathbf{x}}_2)^\top \mathbf{H}(\mathbf{x}_1 - \bar{\mathbf{x}}_2) \right\} \quad (8)$$

defined on $\mathbb{C}^d \times \mathbb{C}^d$, where \bar{x}_2 is the conjugate of x_2 , and \mathbf{H} is an invertible real-valued matrix.

Next, we propose the specific form of $s_t(\mathbf{X}_t; \boldsymbol{\theta}_t)$. An initial thought is to minimize the sample version of the objective function (7) over the space $\mathcal{H}_{\mathcal{K}}^d$ with a ridge penalty, closely mirroring the kernel ridge regression (Zhang et al., 2015; Wainwright, 2019). However, this typically results in nd basis functions at the sample level as in Sriperumbudur et al. (2017) and Zhou et al. (2020) which focus on density estimation without measurement error. The plenty of basis functions make the computation cumbersome. To mitigate this, we propose an alternative way to construct the $s_t(\mathbf{X}_t; \boldsymbol{\theta}_t)$. Under Assumption 3 in Supplementary Material, by invoking (25), we know that $\mathbb{E}[\|\nabla \log p_t(\mathbf{X}_t)\|^2] < \infty$. Then there is a real vector-valued function $\mathbf{f}_t(\cdot)$ satisfying $\nabla \log p_t(\mathbf{x}) = \mathbb{E}_{\mathbf{X}_t}[\mathcal{K}(\mathbf{x}, \mathbf{X}_t)\mathbf{f}_t(\mathbf{X}_t)]$ according to the discussion at the beginning of Section 5 in Smale and Zhou (2003). Moreover, to make this formulation computable, noting that $\mathbf{X}_1 = \mathbf{X}_t + \Sigma^{\frac{1}{2}}(\mathbf{W}_1 - \mathbf{W}_t)$, $\Sigma^{\frac{1}{2}}(\mathbf{W}_1 - \mathbf{W}_t) \sim \mathcal{N}(\mathbf{0}, (1-t)\Sigma)$ and $\Sigma^{\frac{1}{2}}(\mathbf{W}_1 - \mathbf{W}_t) \perp \mathbf{X}_t$, we further have $\nabla \log p_t(\mathbf{x}) = \mathbb{E}_{\xi}[\mathcal{K}(\mathbf{x}, \mathbf{X}_1 + i\sqrt{1-t}\xi)\mathbf{f}_t(\mathbf{X}_t)]$ by combining Lemma 1 and the discussion in above. Thus, the score function $\nabla \log p_t(\cdot)$ can be approximated by the following mean,

$$\nabla \log p_t(\mathbf{x}) \approx \frac{1}{m} \sum_{i=1}^m \mathbf{f}_t(\mathbf{X}_t^{(i)}) \mathbb{E}_{\xi}[\mathcal{K}(\mathbf{x}, \mathbf{X}_1^{(i)} + i\sqrt{1-t}\xi)] = \frac{1}{m} \sum_{i=1}^m \mathbf{f}_t(\mathbf{X}_t^{(i)}) \mathcal{K}_t(\mathbf{x}, \mathbf{X}_1^{(i)}), \quad (9)$$

which only depends on subsample with $m \ll n$ being the size of the subsample,

$$\mathcal{K}_t(\mathbf{x}_1, \mathbf{x}_2) = \sqrt{|\boldsymbol{\Omega}_t|^{-1}|\boldsymbol{\Omega}|} \exp\left\{-\left(\mathbf{x}_1 - \mathbf{x}_2\right)^\top \mathbf{H}_t \left(\mathbf{x}_1 - \mathbf{x}_2\right)\right\} \quad (10)$$

for any real vectors \mathbf{x}_1 and \mathbf{x}_2 , $\boldsymbol{\Omega} = (2\Sigma)^{-1}$, $\boldsymbol{\Omega}_t = \boldsymbol{\Omega} - (1-t)\mathbf{H}$ and $\mathbf{H}_t = \{\mathbf{H}^{-1} - (1-t)\boldsymbol{\Omega}^{-1}\}^{-1}$. The derivation of (10) is in Supplementary Material D.2. Equation (10) motivates us to the basis functions induced by a subsample to approximate the true score function. The use of a subsample instead of the full sample can accelerate the computation. This trick can be viewed as an extension of the random sketch technique adopted in kernel ridge regression which can improve computational efficiency while maintaining the optimal convergence rate (Yang et al., 2017). The choice of m will be discussed in Section 4.2 Next, we study the approximation error of the kernel-based model.

According to (9), we propose to approximate $\nabla \log p_t$ by elements in $\mathcal{H}_{\mathcal{K}_t, m}^d = \mathcal{H}_{\mathcal{K}_t, m} \times \cdots \times \mathcal{H}_{\mathcal{K}_t, m}$ where $\mathcal{H}_{\mathcal{K}_t, m} \subset \mathcal{H}_{\mathcal{K}}$ is the linear span of $\{\mathcal{K}_t(\mathbf{x}, \mathbf{X}_1^{(i)})\}_{i=1}^m$. Besides, we use $\boldsymbol{\theta}_{t, l} =$

$(\theta_{t,l}^{(1)}, \dots, \theta_{t,l}^{(m)})^\top \in \mathbb{R}^m$, $\boldsymbol{\theta}_t = (\boldsymbol{\theta}_{t,1}, \dots; \boldsymbol{\theta}_{t,d}) \in \mathbb{R}^{m \times d}$ to represent parameters in our kernel-based model $\mathbf{s}_t(\mathbf{x}; \boldsymbol{\theta}_t)$ which is defined as

$$\mathbf{s}_t(\mathbf{x}; \boldsymbol{\theta}_t) = (s_{t1}(\mathbf{x}; \boldsymbol{\theta}_t), \dots, s_{td}(\mathbf{x}; \boldsymbol{\theta}_t))^\top, \quad s_{tl}(\mathbf{x}; \boldsymbol{\theta}_t) = \sum_{i=1}^m \theta_{t,l}^{(i)} \mathcal{K}_t(\mathbf{x}, \mathbf{X}_1^{(i)}), \quad (11)$$

for $l = 1, \dots, d$.

Proposition 1. *Under Assumption 3 and 4 in Supplementary Material and B, define*

$$\delta_{0m}(\eta) = 2 \left(\frac{H_0}{m} + \frac{\sigma_0}{\sqrt{m}} \right) \log \left(\frac{2}{\eta} \right),$$

where σ_0, H_0 are the constants in the Bernstein-type concentration condition, Assumption 4. Then,

$$\inf_{\mathbf{s}_t(\cdot; \boldsymbol{\theta}_t) \in \mathcal{H}_{\mathcal{K}_t, m}^d} \mathbb{E}_{\mathbf{X}_t} [\|\mathbf{s}_t(\mathbf{X}_t; \boldsymbol{\theta}_t) - \nabla \log p_t(\mathbf{X}_t)\|^2] \leq 2\delta_{0m}(\eta)^2 + \frac{2\sigma_0^2}{m}$$

holds with probability at least $1 - \eta$ ($0 < \eta < 1$). Here the randomness is from that of $\mathcal{H}_{\mathcal{K}_t, m}^d$.

This proposition shows that the optimal kernel-based model $\mathbf{s}_t(\cdot; \boldsymbol{\theta}_t)$ approximates the desired score function with error less than $\mathcal{O}(1/m)$, which guarantees its effectiveness. The proof of it is in Supplementary Material D.2. Based on the formulation of $\mathbf{s}_t(\cdot; \boldsymbol{\theta}_t)$, the following proposition provides an explicit unbiased estimation of the desired objective (7) to be minimized.

Proposition 2. *With $\mathbf{s}_t(\mathbf{x}; \boldsymbol{\theta}_t)$ defined in (11), an unbiased estimate for the objective (7) is*

$$\text{tr} \left\{ \boldsymbol{\theta}_t^\top \mathbf{K}_t^{(1)} + \boldsymbol{\theta}_t^\top \mathbf{K}_t^{(2)} \boldsymbol{\theta}_t \right\}, \quad (12)$$

where $\mathbf{K}_t^{(1)}$ is a $m \times d$ matrix whose (i, l) -th element equals to $2(n-m)^{-1} \sum_{k=m+1}^n \mathcal{K}_t^{(1,l)}(\mathbf{X}_1^{(k)}; \mathbf{X}_1^{(i)})$,

$\mathbf{K}_t^{(2)}$ is a $m \times m$ matrix whose (i, j) -th element equals to $(n-m)^{-1} \sum_{k=m+1}^n \mathcal{K}_t^{(2)}(\mathbf{X}_1^{(k)}; \mathbf{X}_1^{(i)}, \mathbf{X}_1^{(j)})$,

$$\mathcal{K}_t^{(1,l)}(\mathbf{x}; \mathbf{x}_1) = -2 \frac{|\boldsymbol{\Omega}|}{\sqrt{|\boldsymbol{\Omega}_t| |\boldsymbol{\Omega}_t^{(1)}|}} \mathbf{e}_l^\top \mathbf{H}_t^{(1)}(\mathbf{x} - \mathbf{x}_1) \exp \left\{ -(\mathbf{x} - \mathbf{x}_1)^\top \mathbf{H}_t^{(1)}(\mathbf{x} - \mathbf{x}_1) \right\},$$

and

$$\begin{aligned} \mathcal{K}_t^{(2)}(\mathbf{x}; \mathbf{x}_1, \mathbf{x}_2) &= \frac{|\boldsymbol{\Omega}|^{\frac{3}{2}}}{|\boldsymbol{\Omega}_t| |\boldsymbol{\Omega}_t^{(2)}|^{\frac{1}{2}}} \exp \left\{ -(\mathbf{x}_1 + \mathbf{x}_2 - 2\mathbf{x})^\top \mathbf{H}_t^{(2)}(\mathbf{x}_1 + \mathbf{x}_2 - 2\mathbf{x}) \right\} \\ &\quad \times \exp \left\{ -(\mathbf{x}_1 - \mathbf{x})^\top \mathbf{H}_t(\mathbf{x}_1 - \mathbf{x}) \right\} \\ &\quad \times \exp \left\{ -(\mathbf{x}_2 - \mathbf{x})^\top \mathbf{H}_t(\mathbf{x}_2 - \mathbf{x}) \right\}, \end{aligned}$$

for any \mathbf{x} , \mathbf{x}_1 and \mathbf{x}_2 . Here \mathbf{e}_l is the l -th basis vector in the d -dimensional space, $\Omega_t^{(1)} = \Omega - (1 - t)\mathbf{H}_t$, $\mathbf{H}_t^{(1)} = (1 - t)\mathbf{H}_t\Omega_t^{(1)-1}\mathbf{H}_t + \mathbf{H}_t$, $\Omega_t^{(2)} = \Omega - 2(1 - t)\mathbf{H}_t$ and $\mathbf{H}_t^{(2)} = (1 - t)\mathbf{H}_t\Omega_t^{(2)-1}\mathbf{H}_t$.

The proof to this proposition is in Supplementary Material D. Notably, the expected objective function (7) involves expectation taking w.r.t. \mathbf{X}_1 and $\boldsymbol{\xi}$, whereas due to the formulation of our $s_t(\cdot; \boldsymbol{\theta}_t)$, the expectation w.r.t. $\boldsymbol{\xi}$ can be explicitly computed without requiring a Monte-Carlo approximation. We refer readers for more details to the above discussion in our proof to Proposition 2. Moreover, as in the literature (De Vito et al., 2005; Smale and Zhou, 2003, 2007; Wainwright, 2019), we add a regularization term $\lambda \|s_t(\cdot; \boldsymbol{\theta}_t)\|_{\mathcal{H}_{\mathcal{K}}}^2$ to our training objective (12), where $\lambda > 0$ is a regularization parameter, and $\|s_t(\cdot; \boldsymbol{\theta}_t)\|_{\mathcal{H}_{\mathcal{K}}}$ is the norm of $s_t(\cdot; \boldsymbol{\theta}_t)$ in the d -dimensional RKHS. As discussed in the existing literature related to RKHS, such regularization term is critical to avoid the over-fitting of kernel-based model (Smale and Zhou, 2003, 2007). The scale of selected λ refers to our discussion in Theorem 2. Then, we obtain the *final objective function* for each $\boldsymbol{\theta}_t$,

$$\min_{\boldsymbol{\theta}_t} \text{tr} \left\{ \boldsymbol{\theta}_t^\top \mathbf{K}_t^{(1)} + \boldsymbol{\theta}_t^\top \mathbf{K}_t^{(2)} \boldsymbol{\theta}_t + \lambda \boldsymbol{\theta}_t^\top \mathbf{K}_t^{(0)} \boldsymbol{\theta}_t \right\}, \quad (13)$$

where $\mathbf{K}_t^{(0)}$ is a $m \times m$ matrix whose (i, j) -th element equals to the inner product between $\mathcal{K}_t(\cdot, \mathbf{X}_1^{(i)})$ and $\mathcal{K}_t(\cdot, \mathbf{X}_1^{(j)})$ in $\mathcal{H}_{\mathcal{K}}$,

$$\begin{aligned} \left\langle \mathcal{K}_t(\cdot, \mathbf{X}_1^{(i)}), \mathcal{K}_t(\cdot, \mathbf{X}_1^{(j)}) \right\rangle_{\mathcal{H}_{\mathcal{K}}} &= \mathbb{E}_{\boldsymbol{\xi}, \boldsymbol{\xi}'} \left[\mathcal{K} \left(\mathbf{X}_1^{(i)} + i\sqrt{1-t}\boldsymbol{\xi}, \mathbf{X}_1^{(j)} + i\sqrt{1-t}\boldsymbol{\xi}' \right) \right] \\ &= \sqrt{|\Omega_t^{(0)}|^{-1} |\Omega^{(0)}|} \exp \left\{ - \left(\mathbf{X}_1^{(i)} - \mathbf{X}_1^{(j)} \right)^\top \mathbf{H}_t^{(0)} \left(\mathbf{X}_1^{(i)} - \mathbf{X}_1^{(j)} \right) \right\} \\ &=: \mathcal{K}_t^{(0)} \left(\mathbf{X}_1^{(i)}, \mathbf{X}_1^{(j)} \right). \end{aligned}$$

Here $\Omega^{(0)} = (4\Sigma)^{-1}$, $\Omega_t^{(0)} = \Omega^{(0)} - (1 - t)\mathbf{H}$, $\mathbf{H}_t^{(0)} = \{\mathbf{H}^{-1} - (1 - t)\Omega^{(0)-1}\}^{-1}$, and $\boldsymbol{\xi}$, $\boldsymbol{\xi}'$ are independent random vectors that follow $\mathcal{N}(\mathbf{0}, \Sigma)$. Notably, one should choose \mathbf{H} depends on the variance Σ to ensure that \mathbf{H}_t , $\mathbf{H}_t^{(1)}$, $\mathbf{H}_t^{(2)}$, $\Omega_t^{(0)}$, $\Omega_t^{(1)}$ and $\Omega_t^{(2)}$ are all positive definite, which imposes restrictions on the \mathbf{H} . A rule-of-thumb choice for \mathbf{H} that fulfills the requirement is $\mathbf{H} = (8\Sigma)^{-1}$.

Thereafter, since $\mathbf{K}_t^{(2)}$ is positive semi-definite, the training objective (13) is a convex quadratic programming problem, and its minimizer can be represented as

$$\hat{\boldsymbol{\theta}}_t = -\frac{1}{2}(\mathbf{K}_t^{(2)} + \lambda\mathbf{K}_t^{(0)})\mathbf{K}_t^{(1)}, \quad (14)$$

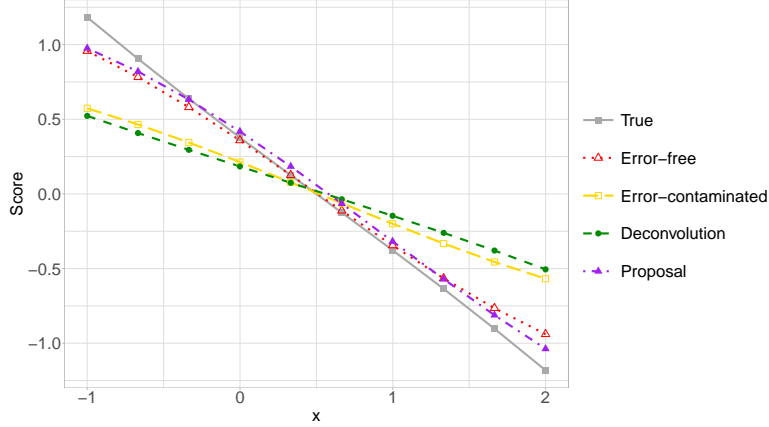


Figure 1: The comparison of score functions fitted using different methods.

where $+$ denotes the Moore–Penrose generalized inverse. Leveraging the estimated score model $s_t(\cdot; \hat{\theta}_t)$, we can generate denoised data by solving reverse SDE (4), which is elaborated in latter.

Finally, we use a simulation in the univariate case to provide some intuitive illustration on the effectiveness of our estimation. Let $n = 1000$, $\epsilon \sim \mathcal{N}(0, 2)$, $X_0 \sim 0.5\mathcal{N}(1, 1) + 0.5\mathcal{N}(0, 1)$, and $X_1 = X_0 + \epsilon$. We set $H = 1/(8 \times 2)$, $m = \lfloor n^{1/2} \rfloor = 31$, and $\lambda = n^{-1/2}$ as suggested by Corollary 2. We compare the estimated score of the proposed method with estimations obtained by three other methods: the score obtained using RKHS-based score matching (Zhou et al., 2020) on top of the error-free and error-contaminated data, respectively, and the deconvolution score function obtained from the density estimated by the R package `deconv` (Wang and Wang, 2011) using the classic kernel smoothing-based deconvolution method (Fan, 1991). As in Figure 1, the proposed method produces a score function close to the ground truth and the score model fitted based on error-free data, which verifies the effectiveness of our complex-value score matching method.

3.3 Sampling with Empirical Reverse-SDE

As mentioned in the above section, the ground truth score function $\nabla \log p_t(\cdot)$ is approximated by $s_t(\cdot; \hat{\theta}_t)$. Then, starting from an error-contaminated observation $\tilde{X}_0 \sim P_{X_1}$ and substituting $\nabla \log p_{1-t}(\tilde{X}_t)$ in (5) with $s_t(\tilde{X}_t; \hat{\theta}_{1-t})$, we can generate a denoised observation through a empirical version of the reverse SDE (4). To do so, we solve (5) by some numerical method. In this paper, we

use $\widehat{\mathbf{X}}_t$ to represent the empirical version of $\widetilde{\mathbf{X}}_t$ which is generated from the following standard first-order Euler-Maruyama (Platen, 1999) sampling method

$$\widehat{\mathbf{X}}_{(k+1)/K} = \widehat{\mathbf{X}}_{k/K} + \frac{1}{K} \boldsymbol{\Sigma} \mathbf{s}_t \left(\widehat{\mathbf{X}}_{k/K}; \widehat{\boldsymbol{\theta}}_{1-k/K} \right) + \sqrt{\frac{1}{K}} \boldsymbol{\Sigma}^{\frac{1}{2}} \boldsymbol{\epsilon}_k, \quad (15)$$

with $\widehat{\mathbf{X}}_0 = \mathbf{X}_1$ as error-contaminated observation, where K is a positive integer represents the step number, $\boldsymbol{\epsilon}_k \sim \mathcal{N}(\mathbf{0}, \mathbf{I})$, and $0 \leq k \leq K - 1$. In practice, we propose to take the error-contaminated observations $\{\mathbf{X}_1^{(i)}\}_{i=1}^n$ as the initialization of (15) to generate n denoised observations.

4 Theoretical Analysis

In the above, we present our method to generate denoised data. However, there is a gap between the distribution of generated $\widehat{\mathbf{X}}_1$ and the desired $P_{\widetilde{\mathbf{X}}_1} = P_{\mathbf{X}_0}$, because 1): There is a difference between the estimated score $\mathbf{s}_t(\cdot; \widehat{\boldsymbol{\theta}}_t)$ and the ground truth score $\nabla \log p_t(\cdot)$ due to the estimation error; 2): The reverse SDE is numerical solved by (15), which leads to discretion error. In this section, we theoretically characterize the gap between the distribution of $\widehat{\mathbf{X}}_1$ and the desired $P_{\mathbf{X}_0}$.

4.1 Discrepancy between the Denoised Data and the Error-free Data

In this section, we establish the upper bound for the sampling error under some mild Assumptions. To do so, we first assume the kernel-based score model $\mathbf{s}_t(\cdot; \widehat{\boldsymbol{\theta}}_t)$ approximates the ground truth score $\nabla \log p_t(\mathbf{x})$ well (we will analyze this approximation error latter in Section 4.2). Our result is presented in the following theorem, which characterizes the gap between the distribution of the generated denoised data $\widehat{\mathbf{X}}_1$ and the desired \mathbf{X}_0 .

Theorem 1. *Suppose the $\widehat{\mathbf{X}}_0 \sim P_{\mathbf{X}_1}$ is independent of $\widehat{\boldsymbol{\theta}}_t$, and $\widehat{\mathbf{X}}_1$ is generated based on the initial point $\widehat{\mathbf{X}}_0$ following the diffusion updates in (15). Under Assumption 3 in Supplementary Material B.2, and assume that for all $t \in [0, 1]$,*

$$\mathbb{E} \left[\left\| \mathbf{s}_t(\mathbf{X}_t; \widehat{\boldsymbol{\theta}}_t) - \nabla \log p_t(\mathbf{X}_t) \right\|^2 \right] \leq \delta. \quad (16)$$

Then,

$$D_{KL} \left(P_{\mathbf{X}_0} \parallel P_{\widehat{\mathbf{X}}_1} \right) = \mathcal{O} \left(\frac{\lambda_{\max}(\boldsymbol{\Sigma}) L_{\text{Tr}}\{\boldsymbol{\Sigma}\}}{K} + \frac{dL\lambda_{\max}^2(\boldsymbol{\Sigma})}{K^2} + \lambda_{\max}(\boldsymbol{\Sigma})\delta \right). \quad (17)$$

We prove this theorem in Supplementary Material E. Theorem 1 indicates that when the score function is well approximated ($\delta \rightarrow 0$), under large sampling steps ($K \rightarrow \infty$), the denoised data distribution $P_{\widehat{\mathbf{X}}_1}$ approximates the target $P_{\mathbf{X}_0}$ well. Thus, the generated denoised data are qualified for downstream tasks such as estimation, prediction, and hypothesis testing. Here, the terms related to step size $1/K$ and estimation error δ , are respectively correspond to the ‘‘discretion error’’ and ‘‘approximation error’’. Intuitively, they appear in (17) because the error between the generated data (15) and ground truth (2) has two origins: 1): The gap between the estimated score function $\mathbf{s}_t(\cdot; \boldsymbol{\theta}_t)$ and the ground truth $\nabla \log p_t(\cdot)$; 2): The discretion error brought by the numerical solver (15).

Notably, by invoking Pinsker’s inequality, we can obtain the following bound for the total variation distance (Wasserman, 2006; Wainwright, 2019)

$$\text{TV} \left(P_{\mathbf{X}_0}, P_{\widehat{\mathbf{X}}_1} \right) \leq \sqrt{\frac{1}{2} D_{KL} \left(P_{\mathbf{X}_0} \parallel P_{\widehat{\mathbf{X}}_1} \right)} = \mathcal{O} \left(\sqrt{\frac{d}{K}} + \delta \right)$$

provided that $\text{tr}(\boldsymbol{\Sigma})$ is $\mathcal{O}(d)$, where $\text{TV} \left(P_{\mathbf{X}_0}, P_{\widehat{\mathbf{X}}_1} \right)$ is the total variation distance defined as

$$\text{TV} \left(P_{\mathbf{X}_0}, P_{\widehat{\mathbf{X}}_1} \right) = \sup_{\mathcal{A} \text{ is measurable}} |P(\mathbf{X}_0 \in \mathcal{A}) - P(\widehat{\mathbf{X}}_1 \in \mathcal{A})|.$$

In our Theorem 1, we assume the independence between the initial point $\widehat{\mathbf{X}}_0$ and the estimate $\widehat{\boldsymbol{\theta}}_t$.¹, which can be guaranteed by a leave-one-out training procedure, i.e., for $i = 1, \dots, n$, training the i -th score model using all data except $\mathbf{X}_1^{(i)}$ and then taking $\mathbf{X}_1^{(i)}$ as the initial point to generate the denoised data by the i -th score model. However, such training suffers from high computational complexity, because we need to train the score models for n times. Alternatively, one can split $\{\mathbf{X}_1^{(i)}\}_{i=m+1}^n$ into two disjoint sets $\mathcal{D}_{\text{train}}$ and \mathcal{D}_{gen} with roughly equal sizes, then train the score model with $\mathcal{D}_{\text{train}}$ and use data in \mathcal{D}_{gen} as the initializations to generate denoised data. This also ensures the independence in Theorem 1 at the cost of reducing the sample size of the denoised data. For such two methods, the imposed small approximation error can be justified by our Corollary 2.

However, in our experiments, we found the procedure without leave-one-out or data splitting, i.e., use $\{\mathbf{X}_1^{(i)}\}_{i=1}^n$ to train the score model and initialize the SDE, performances reasonably

¹Without this assumption, the small estimation condition (16) should be substituted by $\mathbb{E}_{\mathbf{X}_t | \mathbf{X}_1 = \mathbf{X}_1^{(i)}} [\|\mathbf{s}_t(\mathbf{X}_t; \widehat{\boldsymbol{\theta}}_t) - \nabla \log p_t(\mathbf{X}_t)\|^2] \leq \delta$, which is hard to verified. For more details, please check our proof in Supplementary Material E.

well. We conjecture that the independence condition in Theorem 1 can be relaxed to some weak dependence conditions. We did not pursue this because the analysis is rather involved. In practice, we recommend to implementing the proposed method without leave-one-out or data splitting.

4.2 Error Analysis to the Score-Function Model

From Theorem 1, part of the sampling error related to the proposed method originates from the gap between trained model $\mathbf{s}_t(\cdot; \hat{\boldsymbol{\theta}}_t)$ and the ground truth score function $\nabla \log p_t(\cdot)$. Next, we characterize such a gap. To this end, we first introduce some assumptions and definitions. Recall that, for $t \in [0, 1]$, \mathbf{f}_t is the real vector-valued function \mathbf{f}_t such that $\nabla \log p_t(\mathbf{x}) = \mathbb{E}_{\mathbf{X}_t}[\mathcal{K}(\mathbf{x}, \mathbf{X}_t)\mathbf{f}_t(\mathbf{X}_t)]$.

Assumption 1. For $t \in [0, 1]$, $\mathbb{E} \left[\exp \left\{ |\boldsymbol{\Omega}_t^{(0)}|^{-1/2} |\boldsymbol{\Omega}^{(0)}|^{1/2} \|\mathbf{f}_t(\mathbf{X}_1)\|^2 \right\} \right] \leq \exp(B_{\mathcal{K}})$ for some constant $B_{\mathcal{K}} < \infty$.

Assuming that each component of \mathbf{f}_t is bounded, then we have $\sup_{\mathbf{x}} |\boldsymbol{\Omega}_t^{(0)}|^{-1/2} |\boldsymbol{\Omega}^{(0)}|^{1/2} \|\mathbf{f}_t(\mathbf{x})\|^2 = \mathcal{O}(d|\boldsymbol{\Omega}_t^{(0)}|^{-1/2} |\boldsymbol{\Omega}^{(0)}|^{1/2})$. Thus, the constant $B_{\mathcal{K}}$ scales with d at the order of $\mathcal{O}(c^d)$ for some $c > 1$.

Let $\eta > 0$ and $\boldsymbol{\Gamma}_t = \mathbb{E}[\boldsymbol{\Gamma}_{\mathbf{X}_1, t}]$, similar to Proposition 1, define

$$\delta_{1n}(\eta) = 2 \left(\frac{H_1}{n-m} + \frac{\sigma_1}{\sqrt{n-m}} \right) \log \left(\frac{2}{\eta} \right), \quad \delta_{2n}(\eta) = 2 \left(\frac{H_2}{n-m} + \frac{\sigma_2}{\sqrt{n-m}} \right) \log \left(\frac{2}{\eta} \right),$$

and

$$C_{\eta, m, \lambda} = \lambda^{-1} \left\{ \frac{2\sigma_0^2}{m} + 2\delta_{0m}(\eta)^2 \right\} + B_{\mathcal{K}} \log(\eta^{-1}),$$

where σ_1, σ_2, H_1 and H_2 are the constants in Assumption 5 in Supplementary Material B. We have the following non-asymptotic upper bound for $\mathbb{E}_{\mathbf{X}_t}[\|\mathbf{s}_t(\mathbf{X}_t; \hat{\boldsymbol{\theta}}_t) - \nabla \log p_t(\mathbf{X}_t)\|^2]$.

Theorem 2. Suppose $\lambda > 2\delta_{2n}(\eta)$. Under Assumption 1 and Assumption 5 in Supplementary Material B.3, for any $t \in [0, 1]$,

$$\begin{aligned} & \mathbb{E}_{\mathbf{X}_t} \left[\left\| \mathbf{s}_t(\mathbf{X}_t; \hat{\boldsymbol{\theta}}_t) - \nabla \log p_t(\mathbf{X}_t) \right\|^2 \right] \\ & \leq 2\lambda B_{\mathcal{K}} \log(\eta^{-1}) + \frac{4\sigma_0^2}{m} + 4\delta_{0m}(\eta)^2 + \frac{4(\delta_{1n}(\eta) + 2\delta_{2n}(\eta)\sqrt{C_{\eta, m, \lambda}})^2}{\lambda} \end{aligned}$$

holds with probability at least $1 - 4\eta$, where the randomness is from that of $\hat{\boldsymbol{\theta}}_t$.

The proof of this theorem is in Supplementary Material F. By selecting $\lambda \asymp n^{-1/2}$ and $m \asymp n^{1/2}$, Theorem 2 implies that $\mathbb{E}_{\mathbf{X}_t} \left[\|\mathbf{s}_t(\mathbf{X}_t; \hat{\boldsymbol{\theta}}_t) - \nabla \log p_t(\mathbf{X}_t)\|^2 \right] = \mathcal{O}_P \left(\sqrt{\mathcal{B}_K/n} \right)$, which guarantees the convergence of our estimated score function. Then, by combining Theorems 1 and 2, we know that the δ in Theorem 1 is of order $\mathcal{O}((\mathcal{B}_K/n)^{-1/2})$ with high probability. Thus, our proposed method can generate denoised data whose distribution is close to that of error-free data.

Corollary 2. *Suppose $\lambda \asymp n^{-1/2}$, $m \asymp n^{1/2}$, $\lambda > 2\delta_{2n}(\eta)$, K is sufficiently large and $\widehat{\mathbf{X}}_1$ is generated by Theorem 1. Under Assumption 1 and Assumptions in Supplementary Material B,*

$$\text{TV} \left(P_{\mathbf{X}_0}, P_{\widehat{\mathbf{X}}_1} \right) \leq \sqrt{\frac{1}{2} D_{KL} \left(P_{\mathbf{X}_0} \parallel P_{\widehat{\mathbf{X}}_1} \right)} \leq C \left\{ \frac{\mathcal{B}_K \log(\eta^{-1})}{n} \right\}^{1/4},$$

holds with probability at least $1 - 4\eta$ for some constant $C > 0$.

Corollary 2 implies that the distribution function of $\widehat{\mathbf{X}}_1$ converges to that of \mathbf{X}_0 at the rate of $\mathcal{O}_P((\mathcal{B}_K/n)^{1/4})$, which is faster than the convergence rate (polynomial of $1/\log n$) of the classic kernel smoothing-based deconvolution method (Fan, 1991). The convergence rate of the distribution function converts to that of the quantile under suitable regularity conditions (Van der Vaart, 2000). Notably, Assumption 4 in Supplementary Material B implies that the score function can be approximated well by some (infinitely smooth) analytic function according to Proposition 1, which is not required for classic deconvolution methods. A fundamental result from minimax theory (Carroll and Hall, 1988) states that, within the class of densities with bounded derivatives up to order $\alpha > 0$, the minimax optimal rate for nonparametric deconvolution estimator is $(\log n)^{-\alpha/2}$ under normal errors. The slow rate underscores the inherent difficulty of recovering the distribution of \mathbf{X}_0 once normal measurement errors enter the model and necessitates additional assumptions beyond “ α -smoothness” to achieve a better convergence rate.

5 Simulations

The goal of this section is to evaluate the proposed method’s performance in finite samples to generate a synthetic error-free sample within a generative framework that includes covariates and a

random response. This evaluation is conducted under known ground truth, allowing us to assess various aspects of the denoising process and compare alternative methods from the literature. We focus on this scenario because it enables simultaneous evaluation of the model’s capabilities in both unsupervised settings and predictive tasks. Additionally, it allows us to compare the performance of our proposed Algorithm 1 against commonly-used methods in the literature.

Specifically, we generate error-free covariate \mathbf{Z}_0 from the normal mixture $\sum_{i=1}^I w^{(i)} \mathcal{N}(\boldsymbol{\mu}^{(i)}, \boldsymbol{\Sigma}^{(i)})$, where the weights $\{w^{(i)}\}_{i=1}^I$, centers $\{\boldsymbol{\mu}^{(i)}\}_{i=1}^I$, and covariance matrices $\{\boldsymbol{\Sigma}^{(i)}\}_{i=1}^I$ are all randomly generated from normal distributions (weights are normalized using the Softmax function, $\boldsymbol{\Sigma}^{(i)}$ are normalized to be positive definite). We set the number of mixture components to $I = 5$. Additionally, we generate the outcome Y_0 from

$$Y_0 = f_{\boldsymbol{\beta}_{\text{truth}}}(\mathbf{Z}_0) + e_0,$$

where $f_{\boldsymbol{\beta}_{\text{truth}}}(\cdot)$ is a three-layer neural network parameterized by $\boldsymbol{\beta}_{\text{truth}}$, $\boldsymbol{\beta}_{\text{truth}}$ is initialized as in He et al. (2015) and $e_0 \sim \mathcal{N}(0, 0.01)$. Here, we construct error-contaminated data $\mathbf{X}_1 = (\mathbf{Z}_1, Y_1)$ as described in Section 1, with $\boldsymbol{\Sigma} = \sigma^2 \mathbf{I}$ and different σ ’s. Using this error-contaminated data, we apply our diffusion-based Algorithm 1 to obtain the error-free data.

Subsequently, we set the parameters as follows: number of samples $n = 1000$, number of sub-samples $m = 31 \approx \sqrt{n}$, $\lambda = 0.031 \approx n^{-1/2}$, $K = 200$, and $\mathbf{H} = 0.1 \mathbf{I}$ in the Gaussian kernel (8) to satisfy the positive semi-definite conditions discussed in Section 3.2.

Evaluation. We generate an independent test sample $\{\tilde{\mathbf{Z}}_0^{(i)}\}_{i=1}^n$ to assess the quality of the denoised data. Then, we employ the **Maximum Mean Discrepancy (MMD)** (Li et al., 2015) as a statistical distance between samples (see Supplementary Material J). Additionally, we use the **Mean Squared Error (MSE)** to evaluate the estimation of the regression function $f_{\boldsymbol{\beta}_{\text{truth}}}$. For MMD, we compare n denoised data $\{\hat{\mathbf{Z}}_0^{(i)}\}_{i=1}^n$ with the n test data $\{\tilde{\mathbf{Z}}_0^{(i)}\}_{i=1}^n$. Here we use MMD because it is applicable to measure the difference between general distributions and can be directly calculated based on observed data without an intermediate step to estimate the density or

Table 1: The results of MMD and MSE under different methods with varied data dimension d_Z ($\sigma = 0.5$). The other hyperparameters are set as the mentioned before. Our results are averaged over 50 independent runs, and all numbers are multiplied by 1000.

Method	$d_Z = 1$		$d_Z = 2$		$d_Z = 4$		$d_Z = 8$	
	MMD	MSE	MMD	MSE	MMD	MSE	MMD	MSE
Diffusion	5.12	0.61	8.61	0.78	13.26	1.67	15.71	2.53
Deconv	13.12	0.92	17.62	1.23	31.68	3.41	69.42	4.12
Error-Contaminated	16.12	0.71	25.51	1.32	27.12	2.38	30.313	2.89
Error-Free	4.91	0.026	10.31	0.079	11.42	0.121	13.33	0.237

the probability distribution. To verify the practical utility of the generated data, we train a neural network $f_{\hat{\beta}_{\text{diffusion}}}(\cdot)$ with the architecture of $f_{\beta_{\text{truth}}}(\cdot)$ using data pairs $\{(\hat{\mathbf{Z}}_0^{(i)}, \hat{Y}_0^{(i)})\}_{i=1}^n$. We quantify the discrepancy by

$$\frac{1}{n} \sum_{i=1}^n \left\| f_{\beta_{\text{truth}}}(\tilde{\mathbf{Z}}_0^{(i)}) - f_{\hat{\beta}_{\text{diffusion}}}(\tilde{\mathbf{Z}}_0^{(i)}) \right\|^2,$$

which approximates $\mathbb{E}_{\mathbf{Z}_0} \|f_{\beta_{\text{truth}}}(\mathbf{Z}_0) - f_{\hat{\beta}_{\text{diffusion}}}(\mathbf{Z}_0)\|^2$, indicating the divergence between the true model and the approximation. We compare our `Diffusion`, against three baselines in Section 3.2: `Error-Free` (using error-free data $\{(\mathbf{Z}_0^{(i)}, Y_0^{(i)})\}_{i=1}^n$), `Error-Contaminated` (using error-contaminated data $\{(\mathbf{Z}_1^{(i)}, Y_1^{(i)})\}_{i=1}^n$), and `Deconv` utilizing a standard deconvolution method (Fan, 1991). `Error-Free` serves as the oracle method, `Error-Contaminated` ignores measurement errors, and `Deconv` represents the standard approach. We generate n observations from the deconvoluted distribution using rejection sampling when evaluating the MMD of `Deconv`. We present MMD and MSE for all methods in Tables 1 and 2.

Theoretical MMD for `Error-Free` should be zero and the numbers in the Table are non-zero due to sampling variability in the training and testing sample. As can be seen, results in Tables 1 and 2 demonstrate that our `Diffusion` method consistently outperforms `Error-Contaminated` and `Deconv`, approaching the performance of `Error-Free`, particularly at lower noise levels.

Table 2: The results of MMD and MSE under different methods with varied noise level σ ($d_Z = 3$). The other hyperparameters are set as mentioned before. Our results are averaged over 50 independent runs, and all numbers are multiplied by 1000.

Method	$\sigma = 0.1$		$\sigma = \sqrt{0.1}$		$\sigma = 0.5$		$\sigma = \sqrt{0.5}$	
	MMD	MSE	MMD	MSE	MMD	MSE	MMD	MSE
Diffusion	6.91	0.084	7.23	0.38	9.21	0.85	16.27	1.71
Deconv	7.92	0.41	8.71	0.71	18.92	1.36	23.97	1.78
Error-Contaminated	7.83	0.31	8.92	0.47	18.97	0.97	46.12	1.92
Error-Free	6.81	0.046	6.81	0.046	6.81	0.046	6.81	0.046

Notably, at low noise levels and large dimensions, `Error-Contaminated` sometimes achieves better MSE than `Deconv`, likely due to neural networks’ robustness to Gaussian noise (Madry et al., 2017) and the curse of dimensionality issue of kernel smoothing.

Ablation Study We investigate the impact of hyperparameters λ , K , and m in Supplementary Material H. The results indicate that our method remains stable across variations of hyperparameters.

6 Clinical Case Study: Impact of Measurement Error of Glucose Monitors in Diabetes Clinical Trials

Continuous Glucose Monitors (CGMs) are minimally invasive technologies used to record glucose levels over prolonged periods, such as days and weeks. Since their adoption nearly 20 years ago in clinical practice, the benefits of CGMs in managing type 1 diabetes and evaluating the efficacy of new drugs in diabetes trials have become clear. More recently, CGMs have also found novel applications, for example, in human nutrition to support personalized diet prescriptions. Moreover, CGMs are increasingly popular in epidemiological studies involving healthy populations.

Despite their utility, CGMs are subject to significant measurement errors, which can affect the

conclusions drawn from the data, such as those in clinical trials. Although the measurement error of CGM technologies has decreased over time—e.g., the mean absolute relative difference has dropped from approximately 20% to about 10%—it can still be large enough to lead to misleading conclusions about a patient’s real metabolic status and its evolution.

From a technological perspective, understanding the limitations and potential of CGMs in relation to measurement error through novel statistical methods is a major challenge, particularly for regulatory approvals (e.g., from the FDA) of predictive AI algorithms or for defining novel digital biomarkers. Our denoising diffusion framework provides an effective approach to performing sensitivity analyses on how measurement error affects the estimation of possibly complicated digital health metrics and, ultimately, clinical decision-making. The analysis goals of this section are to: i) Use denoising diffusion algorithms to estimate individual distributional representations of CGM data under measurement error; ii) Incorporate denoising steps to enable sensitivity analyses that evaluate new clinical interventions in clinical trials, taking into account the underlying noise level. We focus on assessing statistical inference when comparing two different interventions.

6.1 Data Structure and Collection

Consider n individuals, each with n_i glucose observations collected at times $s^{(i,j)}$, giving pairs $\{(s^{(i,j)}, G^{(i,j)})\}_{j=1}^{n_i}$. Let $X^{(i)}(s)$ be the unobserved glucose process for the i -th individual, where $s \in [0, \mathcal{S}^{(i)}]$. The observed measurements satisfy $G^{(i,j)} = X^{(i)}(s^{(i,j)}) + \epsilon^{(i,j)}$, where $\epsilon^{(i,j)} \sim \mathcal{N}(0, \sigma_0^2)$ and are i.i.d. across all i, j . Though this may be simplistic for real continuous glucose monitoring (CGM) data, it provides a tractable framework for assessing measurement error sensitivity.

From a population perspective, we focus on the marginal distribution of $X^{(i)}(\cdot)$. Define

$$F^{(i)}(s) = \frac{1}{\mathcal{S}^{(i)}} \int_0^{\mathcal{S}^{(i)}} \mathbf{1}\{X^{(i)}(u) \leq s\} du, \quad s \in [40, 400].$$

Various metrics, such as time in hypoglycemia, time in range (TIR), and time in hyperglycemia, can be derived from $F^{(i)}(\cdot)$. We often categorize glucose readings as $G^{(i,j)} \leq 70$ (hypoglycemia), $70 < G^{(i,j)} \leq 180$ (TIR), or $G^{(i,j)} > 180$ (hyperglycemia). In particular, the hypoglycemia,

TIR and hyperglycemia proportions are $\text{Hypo}^{(i)} = F^{(i)}(70)$, $\text{TIR}^{(i)} = F^{(i)}(180) - F^{(i)}(70)$ and $\text{Hyper}^{(i)} = 1 - F^{(i)}(180)$, respectively. For estimation, denoised observations $\{G^{(\sigma,i,j)}\}_{i,j}$ can be used, where $\sigma = 0$ corresponds to the raw measurements ($G^{(0,i,j)} = G^{(i,j)}$). In addition to discrete summaries, we also consider the functional “glucodensity” profile (Matabuena et al., 2021), a density estimator that, in practice, can be estimated via kernel-based methods.

Our overarching goal is to quantify how measurement error affects these population-level CGM metrics and to develop estimators that minimize the related discrepancies. Statistically, we assume that the population cdf $F^{(i)}(\cdot)$ corresponds to a continuous-time stochastic process $X^{(i)}(\cdot)$ that is “slowly varying” or approximately stationary during the observational window. From a biological perspective—especially in diseases like diabetes—it is reasonable to assume that the metabolic evolution of the disease is not rapid so that the distribution $F^{(i)}(\cdot)$ remains roughly time-invariant over the study period. Summarizing this distributional behavior via the marginal cdf $F^{(i)}(\cdot)$ is therefore a good proxy for tracking glucose health patterns and a good method to predict long-term diabetes outcomes (Matabuena et al., 2024a).

6.2 Data Description

Our study is motivated by data from the JDRF CGM Study Group (Tamborlane et al., 2008; JDRF CGM Study Group, 2009), an early large-scale clinical trial evaluating CGM for managing type 1 diabetes (T1DM). Data were obtained from the multi-center trial², wherein 451 adults and children were randomized to either a CGM-based (treatment) arm or a standard-of-care (control) arm.

For this analysis, we focus on 188 individuals (102 control, 86 treatment) with minimal missing CGM data at the study’s start and end of the intervention. We focus on CGM-based measures (time in hypo-, hyper-, or time in range) and how they are affected by the measurement error in the underlying glucose process. Note that these CGM metrics are among the current state-of-the-art metrics promoted by the American Diabetes Association.

²JDRF CGM RCT, NCT00406133; <https://public.jaeb.org/datasets/diabetes>

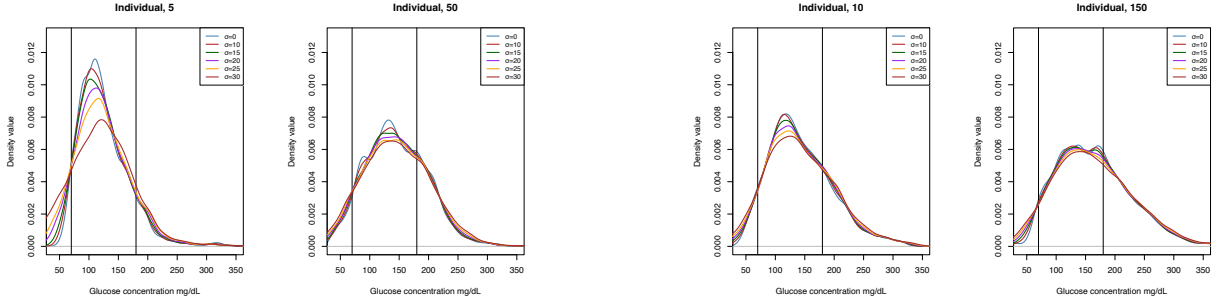
6.3 Density Function Estimation with Measurement Error

Given a noise level σ , and each individual $i = 1, \dots, n$, using the denoising framework, we generate the sample $G^{(\sigma,i,j)}$ for $j = 1, \dots, n_i$. We estimate the marginal density of $\{G^{(\sigma,i,j)}\}_{j=1}^{n_i}$ for each individual by kernel density estimator as in Matabuena et al. (2024a). Figure 2 shows the density estimators for four individuals at noise levels $\sigma = 0, 10, 15, 20, 25, 30$. The first two individuals belong to the control group, and the last two belong to the treatment group at the beginning of the study. We estimate the corresponding densities at both the beginning and end of the interventions. We can appreciate that different noise levels result in varying shapes of the density functions, which can impact the proportion of time spent in clinically relevant target zones defined previously.

To display these conclusions with higher resolution for noise levels $\sigma = 0, 10, 20$, Figure in Supplementary Material K illustrates the variations in the control and treatment groups (RT-CGM) before and after interventions. For example, when comparing $\sigma = 0$ versus $\sigma = 20$ in the boxplot for low glucose concentration (hypoglycemia) and high glucose concentration (hyperglycemia), the median range of variation increases to 1.5 and 0.75, respectively. Although there are certain original variations, for the case of TIR (normal glucose concentration), the estimation reduces by approximately 3% of the time, indicating that the original estimation overestimated the proportion of time that individuals spend within this range. From a clinical point of view, a variation in the hypo- or hyperglycemia proportion of 0.5% can be clinically relevant, especially in hypoglycemia, to detect statistically significant differences in the context of randomized clinical trials.

6.4 Impact of Measurement Error in Intervention Assessment

Now, we focus on the changes in the control and treatment groups (RT-CGM) after the interventions regarding the metrics: hypoglycemia (hypo), hyperglycemia (hyper), and Time in Range (TIR). We consider a boxplot of the differences for each patient after and at the beginning of the intervention. Figure 3 shows these results along with the corresponding p-values derived from a paired t-test for different noise levels $\sigma = 10, 15, 20, 25, 30$. In the case of the hypoglycemia metric for different



(a) Control group

(b) Treatment group

Figure 2: Density estimators for four individuals at different noise levels $\sigma = 0, 10, 15, 20, 25, 30$ at the beginning of the study.

noise levels, there are no statistically significant differences, similar to the TIR metrics. However, the p-values are highly unstable, and the boxplots indicate important changes in the distribution across different noise levels σ . In the case of hyperglycemia (hyper), the p-values are statistically significant except at a noise level of $\sigma = 25$, indicating that changes in noise level can lead to the acceptance or rejection of the null hypothesis at the classical threshold of 0.05, thereby compromising the validation of the positive effect of the interventions.

We recognize that there can be an estimation error between the distributions of the denoised data and the model-free ones even when σ is correctly specified, and the theoretical validity of the t-test p-values needs further justification. However, the p-values and the boxplots under different σ values are always useful for sensitivity analysis of the impact of measurement error in the clinical study.

7 Discussion

This paper proposes a novel statistical machine-learning approach to address the measurement error problem in both supervised and unsupervised data analysis tasks. Our main methodological contribution is an RKHS-based, complex-valued score matching method for training a diffusion model without requiring access to intermediate error-contaminated data. In addition, we provide a theoretical guarantee on the distributional gap between the denoised data and their model-free

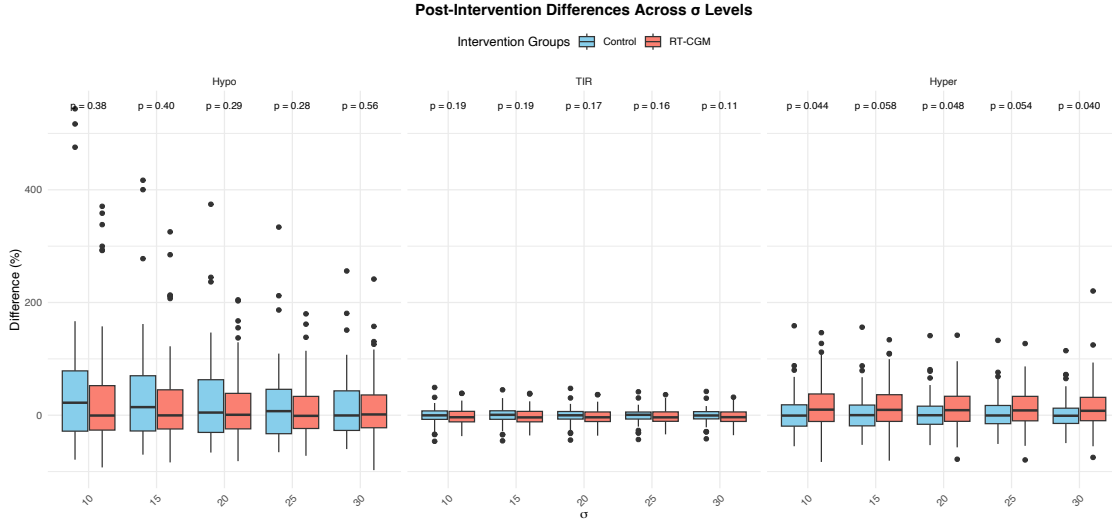


Figure 3: Boxplots of the differences in hypoglycemia (Hypo), hyperglycemia (Hyper), and Time in Range (TIR) metrics for control and treatment groups (RT-CGM) before and after interventions across various noise levels ($\sigma = 10, 15, 20, 25, 30$). The figure also displays corresponding p-values from paired t-tests, indicating the deviation for the null hypothesis for different noise levels.

counterparts. Empirical results support these theoretical findings and demonstrate the effectiveness of our approach for multivariate data. We also present a clinical application in digital health, specifically glucose monitoring, to illustrate the impact of measurement-error modeling on final decision-making. This example highlights the need, in this AI era, to address not only predictive performance but also technological limitations regarding measurement reliability (Bent et al., 2020). Such considerations are particularly relevant for new regulatory agencies (e.g., the FDA) seeking to understand both the potential and the limitations of emerging technologies. Our framework can be applied to various clinical scenarios, including biomarker discovery and the validation of novel therapies. Notably, it can generate denoised data that are readily analyzed with standard statistical techniques, thereby enhancing both interpretability and usability. Furthermore, this flexibility enables practitioners to select the most suitable models for their specific needs.

A natural future research direction for our method is to validate finite-sample performance in supporting statistical inference for parameter estimation. For instance, one can construct confidence

intervals for parameter estimates by using denoised data, which can provide asymptotically valid inferences under suitable conditions. Moreover, through additional resampling techniques—such as generalizing smoothing bootstrap methods to our RKHS-based denoising setting—finite-sample performance can be further improved. Extensions along these lines, including specialized predictive approaches (e.g., conformal prediction) that offer non-asymptotic guarantees, are critical for ensuring trustworthiness in machine learning applications. We view this paper as an initial step toward tackling measurement error using diffusion models. Specifically, we assume that the measurement error follows a normal distribution with a known variance. As a promising direction for future research, we plan to extend this method to accommodate other known or unknown error distributions using diffusion models.

Appendix

A Further Related Work

Measurement error. Data science methods for error-contaminated data have a long history, dating back at least to the early days of econometrics (e.g., Frisch (1934); see Schennach (2016) for a review). Research in this area has remains active and has even gained momentum in recent years. One reason for this renewed interest is the push to relax many standard assumptions (such as linearity and independence), which has led to more complex methodological developments. For examples, the fruitful results in binary regression (Chen et al., 2011), generalized linear models (Stefanski and Carroll, 1987), instrumental variable models (Jiang and Ding, 2020), and survival analysis (Prentice, 1982; Yan and Yi, 2015). However, many of the existing measurement error methods (Loh and Wainwright, 2012; Jiang et al., 2023) are highly model-dependent, which makes them hard to use when the form of the ground truth model is unknown.

Another standard model-free method is deconvolution, which has been developed to estimate the density of the error-free variable when observations are error-contaminated (Fan, 1991; Hall and Maiti, 2009; Belomestny and Goldenshluger, 2021), without requiring the structure of the model. Within this framework, kernel smoothing techniques are employed to estimate the density of the error-free data. However, a significant limitation hampers existing deconvolution techniques: the curse of dimensionality. This issue severely restricts their utility for tasks involving moderate to high dimensions variables.

Diffusion Model. As introduced in Section 1, the diffusion model is proposed as a generative model in AI, which has gained a great success in image generation (Ho et al., 2020; Song et al., 2020b; Rombach et al., 2022; Yi et al., 2023a, 2024); video generation (Ma et al., 2024; Zheng et al., 2024); text generation (Lin et al., 2023; Li et al., 2022). Theoretically, this method is first originated from the Langevin dynamics (Welling and Teh, 2011) to sampling from target distribution, by invoking the technique of score function estimation (Hyvärinen and Dayan, 2005; Vincent, 2011).

Latter, it is linked to VAE (Kingma and Welling, 2013; Sohl-Dickstein et al., 2015; Song et al., 2020a) and widely applied in AI by modeling the score function with proper deep neural network (Ronneberger et al., 2015; Peebles and Xie, 2023).

In the diffusion model, the key idea is transferring a distribution that can be easily sampled into a target one. Therefore, it is quite suitable to tackle the measurement error discussed in this paper, when setting the target distribution as the denoise one as we did in this paper. Though there exists such equivalence, to the best of our knowledge, applying the diffusion model to tackle measurement error has not been explored before this paper. We speculate the main obstacle is correctly estimating the score function of intermediate data. In the diffusion model, the most similar topic to this paper is learning from “corrupted data” (Kawar et al., 2023; Daras et al., 2024), whereas both the error-free data and some data with corruption are observed. Their goal is restoring the corrupted data, which is quite similar to removing the measurement error discussed in this paper. However, for learning from corrupted data, the error-free data is supposed to be observed, so that the score function can be directly estimated based on them. Unfortunately, these error-free data are missing in our regime, so none of their methods can be applied here.

Learning in Reproducing Kernel Hilbert Spaces. Statistical learning in Reproducing Kernel Hilbert Spaces (RKHS) has a rich history in both statistical science and machine learning. The foundations of this area can be traced back to non-linear prediction research by Wahba Wahba (1990), which introduced the idea of learning complex regression functions without explicitly tuning the underlying smoothing hyperparameters. Examples of such methods include kernel ridge regression and support vector machines (Hofmann et al., 2008).

Another important research direction focuses on kernel mean embeddings (Muandet et al., 2017), a technique that maps probability distributions into an RKHS as random elements of that space. Kernel mean embeddings are widely used for comparing distributions (e.g., in two-sample testing), clustering (Matabuena et al., 2022), evaluating generative models, and, more recently, in conformal prediction (Matabuena et al., 2024b). Novel RKHS-based methods have also been proposed for

density estimation (Zhou et al., 2020; Kim and Scott, 2012; Schuster et al., 2020).

Despite the many ways in which the properties of RKHS can be leveraged for data analysis, to the best of our knowledge, there are currently no methods for efficiently handling measurement error while preserving a probability distribution perspective that exploits diffusion models. The intersection of these two fields has the potential to enable powerful, model-free approaches for addressing error in statistical analysis.

B Regularity Conditions

B.1 Standard Regularity Conditions

In this paper, our results are built on the following mild assumptions. They are standard ones in the existing diffusion-based literature (Song et al., 2021).

Assumption 2. *We make the following assumptions through this paper.*

1. For $t \in [0, 1]$, $p_t(\mathbf{x}) \in \mathcal{C}^2$ ³, and $\mathbb{E}[\|\mathbf{X}_t\|^2] < \infty$.
2. $\lambda_{\max}(\Sigma)$ and $\lambda_{\max}(\mathbf{H})$ are bounded from above, $\lambda_{\min}(\Sigma)$ and $\lambda_{\min}(\mathbf{H})$ are bounded from below⁴.
3. There exists positive constant C such that for all \mathbf{x} and $t \in [0, 1]$, it holds $\|\nabla \log p_t(\mathbf{x})\| \leq C(1 + \|\mathbf{x}\|)$.
4. *Novikov's condition.* $\mathbb{E}_{\mathbf{X}_t} \left[\frac{1}{2} \int_0^1 \exp \left(\left\| \Sigma^{\frac{1}{2}} (\nabla_{\mathbf{x}} \log p_t(\mathbf{X}_t) - \hat{\mathbf{s}}_t(\mathbf{X}_t)) \right\|^2 \right) dt \right] < \infty$

Here we make some discussion on these imposed assumptions. For the first, it is a standard moment assumption and the continuity of density of p_t . For the second, it requires the bounded (upper and lower) eigenvalues of Σ and \mathbf{H} . The third condition is imposed to make the reverse-time SDE (5) have a solution (Oksendal, 2013)⁵. The Novikov's condition is a standard one during

³Differentiable function with continuous second order derivative.

⁴Here $\lambda_{\max}(\cdot)$ and $\lambda_{\min}(\cdot)$ are respectively the biggest and the smallest eigenvalues of a matrix.

⁵This assumption is also implied by our Assumption 3.

analyzing the sampling error of diffusion-based model (Song et al., 2021; Lee et al., 2022; Chen et al., 2022), it can be verified if we impose some sub-Gaussian type condition to \mathbf{X}_0 (e.g., \mathbf{X}_0 has bounded support). This is because $\nabla_{\mathbf{x}} \log p_t(\mathbf{X}_t) = \frac{\Sigma^{-1}(\mathbb{E}[\mathbf{X}_0|\mathbf{X}_t] - \mathbf{X}_t)}{t^2}$ from Tweedie's formula (Efron, 2011), and the formulation of our kernel-based model $\hat{\mathbf{s}}$.

B.2 Continuity Condition

Next, we give the continuity assumptions to derive our Theorem 1.

Assumption 3. For any \mathbf{x} and t , the score-function $\nabla_{\mathbf{x}} \log p_t(\mathbf{x})$ and our obtained kernel-based model $\mathbf{s}_t(\mathbf{x}; \hat{\boldsymbol{\theta}}_t)$ are all Lipschitz continuous w.r.t. \mathbf{x} with coefficient L , that says,

$$\begin{aligned} \|\nabla_{\mathbf{x}} \log p_t(\mathbf{x}) - \nabla_{\mathbf{x}} \log p_t(\mathbf{y})\| &\leq L\|\mathbf{x} - \mathbf{y}\|; \\ \|\mathbf{s}_t(\mathbf{x}; \hat{\boldsymbol{\theta}}_t) - \mathbf{s}_t(\mathbf{y}; \hat{\boldsymbol{\theta}}_t)\| &\leq L\|\mathbf{x} - \mathbf{y}\|. \end{aligned}$$

For this condition, we have the following discussion. Firstly, this is a standard condition in the existing literature to conduct error analysis to diffusion-based methods, e.g., (Chen et al., 2022; Lee et al., 2022; Chen et al., 2023; Li et al., 2024). For the second, which is correct under bounded $\hat{\boldsymbol{\theta}}_t$, properly chosen \mathbf{H} in kernel $\mathcal{K}(\mathbf{x}, \mathbf{y})$, due to the formulation of our score model.

B.3 Conditions for Concentration

More than the aforementioned conditions, we further require the following Bernstein-type conditions to derive our concentration results Proposition 1 and Theorem 2.

Before illustrating these conditions, we need some definitions to simplify the notations. For any $\mathbf{x} \in \mathbb{R}^d$, let $\zeta_{\mathbf{x},t} = -2\mathbb{E}_{\boldsymbol{\xi}} [\nabla_{\mathbf{x}} \mathcal{K}(\cdot, \mathbf{x} + i\sqrt{1-t}\boldsymbol{\xi})] \in \mathcal{H}_{\mathcal{K}}^d$ and define the linear operator $\Gamma_{\mathbf{x},t}(\mathbf{s}) = \mathbb{E}_{\boldsymbol{\xi}} [\mathcal{K}(\cdot, \mathbf{x} + i\sqrt{1-t}\boldsymbol{\xi})\mathbf{s}(\mathbf{x} + i\sqrt{1-t}\boldsymbol{\xi})]$ for any $\mathbf{s} \in \mathcal{H}_{\mathcal{K}}^d$. We use $\|\cdot\|_{\text{HS}}$ to denote the Hilbert-Schmidt norm of an operator.

Assumption 4. For $t \in [0, 1]$, \mathbf{f}_t satisfying $\mathbb{E}_{\mathbf{X}_t} [\mathbf{f}_t(\mathbf{X}_t)\mathcal{K}(\mathbf{x}, \mathbf{X}_t)] = \nabla \log p_t(\mathbf{x})$, it holds that

$$\mathbb{E}_{\mathbf{X}'_t, \mathbf{X}'_1} \left[\|\mathbf{f}_t(\mathbf{X}'_t)\mathcal{K}_t(\mathbf{X}_t, \mathbf{X}'_1) - \nabla \log p_t(\mathbf{X}_t)\|_{L^2(P_{\mathbf{X}_t})}^k \right] \leq \frac{k! \sigma_0^2 H_0^{k-2}}{2},$$

for any $k \geq 2$, and some universal constants σ_0 and H_0 , where $\mathbf{X}'_t \sim P_{\mathbf{X}_t}$ for $t \in [0, 1]$ is a process independent of \mathbf{X}_t , and $L_2(P_{\mathbf{X}_t})$ is the L_2 -norm under probability measure $P_{\mathbf{X}_t}$.

Assumption 5. For $t \in [0, 1]$, it holds that

$$\mathbb{E}_{\mathbf{X}_1} \left[\|\zeta_{\mathbf{X}_1, t} - \mathbb{E}_{\mathbf{X}_1}[\zeta_{\mathbf{X}_1, t}]\|_{\mathcal{H}_{\mathcal{K}}^d}^k \right] \leq \frac{k! \sigma_1^2 H_1^{k-2}}{2}$$

and

$$\mathbb{E}_{\mathbf{X}_1} \left[\|\Gamma_{\mathbf{X}_1, t} - \mathbb{E}_{\mathbf{X}_1}[\Gamma_{\mathbf{X}_1, t}]\|_{\text{HS}}^k \right] \leq \frac{k! \sigma_2^2 H_2^{k-2}}{2}$$

for any $k \geq 2$, and some universal constants σ_1 , H_1 , σ_2 and H_2 .

Assumptions 4 and 5 are similar to the conditions required for the concentration results in De Vito et al. (2005); Smale and Zhou (2003, 2007); Zhou et al. (2020), and are commonly used in existing literature of RKHS.

C Discussion on Reverse-Time SDE (5)

Proposition 3. Under Assumption 2, $\widetilde{\mathbf{X}}_t$ in (5) has the same distribution with the solution of SDE (4).

Proof. By Fokker-Planck equation (Oksendal, 2013), we know that the density of SDE (4) follows the PDE

$$\frac{\partial}{\partial t} p_t(\mathbf{x}) = \frac{1}{2} \sum_{i,j=1}^n \sigma_{ij} \frac{\partial^2 p_t(\mathbf{x})}{\partial \mathbf{x}_i \partial \mathbf{x}_j} = \nabla \cdot \left(p_t \frac{\Sigma \nabla \log p_t(\mathbf{x})}{2} \right).$$

Thus we can conclude that \mathbf{X}_t has the same density with the following stochastic ODE \mathbf{x}_t such that

$$d\mathbf{x}_t = \frac{1}{2} \Sigma \nabla \log p_t(\mathbf{x}_t) dt$$

with $\mathbf{x}_0 = \mathbf{X}_0$. Then, due to the reversibility of ODE, we know that \mathbf{x}_t has the same distribution with its reverse-time version $\tilde{\mathbf{x}}_{1-t}$

$$d\tilde{\mathbf{x}}_t = \frac{1}{2} \Sigma \nabla \log p_{1-t}(\tilde{\mathbf{x}}_t) dt, \tag{18}$$

and $p_{1-t}(\cdot)$ serves as the density of $\widetilde{\mathbf{X}}_t$. Then, its F-P equation is replaced with

$$\begin{aligned}\frac{\partial}{\partial t}p_{1-t}(\mathbf{x}) &= -\nabla \cdot \left(p_{1-t}(\mathbf{x}) \frac{\Sigma \nabla \log p_{1-t}(\mathbf{x})}{2} \right) \\ &= -\nabla \cdot (p_{1-t}(\mathbf{x}) \Sigma \nabla \log p_{1-t}(\mathbf{x})) + \frac{1}{2} \sum_{i,j=1}^n \sigma_{ij} \frac{\partial^2 p_{1-t}(\mathbf{x})}{\partial x_i \partial x_j},\end{aligned}$$

which is exactly the F-P equation of reverse SDE (5). Thus, we can conclude that $\mathbf{X}_t \sim \mathbf{x}_t \sim \tilde{\mathbf{x}}_{1-t} \sim \widetilde{\mathbf{X}}_{1-t}$ (“ \sim ” means two random variables have same distribution), which proves the conclusion in Section 3.1. It indicates that $P_{\mathbf{X}_{1-t}} = P_{\widetilde{\mathbf{X}}_t}$ due to the Fokker-Planck equation (Oksendal, 2013). \square

D Proofs for Results in Section 3

D.1 Proof for Results in Section 3.1

Restatement of Corollary 1. *Let $\boldsymbol{\xi} \sim \mathcal{N}(\mathbf{0}, \Sigma)$ be a random vector independent of \mathbf{X}_0 and ϵ . If $\mathbf{s}_t(\mathbf{X}_t; \boldsymbol{\theta}_t)$ and $\nabla \mathbf{s}_t(\mathbf{X}_t; \boldsymbol{\theta}_t)$ are both analytic, then we have*

$$\begin{aligned}\mathbb{E}_{\mathbf{X}_t} \left[\|\mathbf{s}_t(\mathbf{X}_t; \boldsymbol{\theta}_t)\|^2 \right] + 2\text{tr} \{ \mathbb{E}_{\mathbf{X}_t} [\nabla \mathbf{s}_t(\mathbf{X}_t; \boldsymbol{\theta}_t)] \} &= \\ \mathbb{E}_{\mathbf{X}_1, \boldsymbol{\xi}} \left[\|\mathbf{s}_t(\mathbf{X}_1 + i\sqrt{1-t}\boldsymbol{\xi}; \boldsymbol{\theta}_t)\|^2 \right] + 2\text{tr} \{ \mathbb{E}_{\mathbf{X}_1, \boldsymbol{\xi}} [\nabla \mathbf{s}_t(\mathbf{X}_1 + i\sqrt{1-t}\boldsymbol{\xi}; \boldsymbol{\theta}_t)] \},\end{aligned}$$

where $i = \sqrt{-1}$ is the imaginary unit.

Proof. For \mathbf{X}_1 , we can decompose it as $\mathbf{X}_1 = \mathbf{X}_0 + t\boldsymbol{\xi}_1 + \sqrt{1-t}\boldsymbol{\xi}_2$, for any $t \in [0, 1]$ with $\boldsymbol{\xi}_1$ and $\boldsymbol{\xi}_2$ are independent identically distributed normal vector $\mathcal{N}(0, \Sigma)$. W.o.l.g., using analytic function $\|\mathbf{s}(\mathbf{x}, \boldsymbol{\theta}_t)\|^2$ as an example, we have

$$\begin{aligned}\mathbb{E} \left[\|\mathbf{s}(\mathbf{X}_1 + i\sqrt{1-t}\boldsymbol{\xi}; \boldsymbol{\theta}_t)\|^2 \right] &= \mathbb{E} \left[\mathbb{E} \left[\|\mathbf{s}(\mathbf{X}_1 + i\sqrt{1-t}\boldsymbol{\xi}; \boldsymbol{\theta}_t)\|^2 \mid \mathbf{X}_0, \boldsymbol{\xi}_1 \right] \right] \\ &= \mathbb{E} \left[\mathbb{E} \left[\|\mathbf{s}(\mathbf{X}_0 + t\boldsymbol{\xi}_1 + \sqrt{1-t}\boldsymbol{\xi}_2 + i\sqrt{1-t}\boldsymbol{\xi}; \boldsymbol{\theta}_t)\|^2 \mid \mathbf{X}_0, \boldsymbol{\xi}_1 \right] \right] \\ &\stackrel{a}{=} \mathbb{E} \left[\mathbb{E} \left[\|\mathbf{s}(\mathbf{X}_0 + t\boldsymbol{\xi}_1; \boldsymbol{\theta}_t)\|^2 \right] \right] \\ &= \mathbb{E} \left[\mathbb{E} \left[\|\mathbf{s}(\mathbf{X}_t; \boldsymbol{\theta}_t)\|^2 \right] \right],\end{aligned}$$

where the equality a is due to Lemma 1, and the independence between $\mathbf{X}_0, \boldsymbol{\xi}, \boldsymbol{\xi}_1, \boldsymbol{\xi}_2$. Then, we prove our conclusion. The proof is similarly generalized to $\text{tr}\{\nabla \mathbf{s}(\mathbf{x}; \boldsymbol{\theta}_t)\}$. \square

D.2 Proofs for Results in Section 3.2

Restatement of Proposition 1. *Under Assumption 3 and 4 in Supplementary Material and B, define*

$$\delta_{0m}(\eta) = 2 \left(\frac{H_0}{m} + \frac{\sigma_0}{\sqrt{m}} \right) \log \left(\frac{2}{\eta} \right),$$

where σ_0, H_0 are the constants in the Bernstein-type concentration condition, Assumption 4. Then,

$$\inf_{\mathbf{s}_t(\cdot; \boldsymbol{\theta}_t) \in \mathcal{H}_{\mathcal{K}_t, m}^d} \mathbb{E}_{\mathbf{X}_t} [\|\mathbf{s}_t(\mathbf{X}_t; \boldsymbol{\theta}_t) - \nabla \log p_t(\mathbf{X}_t)\|^2] \leq 2\delta_{0m}(\eta)^2 + \frac{2\sigma_0^2}{m}$$

holds with probability at least $1 - \eta$ ($0 < \eta < 1$). Here the randomness is from that of $\mathcal{H}_{\mathcal{K}_t, m}^d$.

Proof. Define

$$\begin{aligned} h(\{\mathbf{X}_t^{(i)}\}_{i=1}^m, \{\mathbf{X}_1^{(i)}\}_{i=1}^m) &= \mathbb{E}_{\mathbf{X}_t} \left[\left\| \frac{1}{m} \sum_{i=1}^m \mathbf{f}(\mathbf{X}_t^{(i)}) \mathcal{K}_t(\mathbf{X}_t, \mathbf{X}_1^{(i)}) - \nabla \log p_t(\mathbf{X}_t) \right\|^2 \right]^{\frac{1}{2}} \\ &= \left\| \frac{1}{m} \sum_{i=1}^m \mathbf{f}(\mathbf{X}_t^{(i)}) \mathcal{K}_t(\mathbf{X}_t, \mathbf{X}_1^{(i)}) - \nabla \log p_t(\mathbf{X}_t) \right\|_{L^2(P_{\mathbf{X}_t})}. \end{aligned}$$

Notice that

$$\inf_{\mathbf{s}_t(\cdot; \boldsymbol{\theta}_t) \in \mathcal{H}_{\mathcal{K}_t, m}^d} \mathbb{E}_{\mathbf{X}_t} [\|\mathbf{s}_t(\mathbf{X}_t; \boldsymbol{\theta}_t) - \nabla \log p_t(\mathbf{X}_t)\|^2] \leq h^2(\{\mathbf{X}_t^{(i)}\}_{i=1}^m, \{\mathbf{X}_1^{(i)}\}_{i=1}^m)$$

by definition. It suffices to establish the high probability upper bound for $h(\{\mathbf{X}_t^{(i)}\}_{i=1}^m, \{\mathbf{X}_1^{(i)}\}_{i=1}^m)$ in order to proof the proposition. Let

$$h_i = \mathbb{E} \left[h(\{\mathbf{X}_t^{(i)}\}_{i=1}^m, \{\mathbf{X}_1^{(i)}\}_{i=1}^m) \mid \mathcal{F}_i \right] - \mathbb{E} \left[h(\{\mathbf{X}_t^{(i)}\}_{i=1}^m, \{\mathbf{X}_1^{(i)}\}_{i=1}^m) \mid \mathcal{F}_{i-1} \right],$$

where \mathcal{F}_i is the σ -field generated by $\{\{\mathbf{X}_t^{(j)}\}_{j=1}^i, \{\mathbf{X}_1^{(j)}\}_{j=1}^i\}$. Then

$$h(\{\mathbf{X}_t^{(i)}\}_{i=1}^m, \{\mathbf{X}_1^{(i)}\}_{i=1}^m) - \mathbb{E}_{\{\mathbf{X}_t^{(i)}\}_{i=1}^m, \{\mathbf{X}_1^{(i)}\}_{i=1}^m} \left[h(\{\mathbf{X}_t^{(i)}\}_{i=1}^m, \{\mathbf{X}_1^{(i)}\}_{i=1}^m) \right] = \sum_{i=1}^m h_i,$$

with $\mathbb{E}[h_i] = 0$, and h_i is martingale difference w.r.t. \mathcal{F}_k . Besides that, by defining

$$\begin{aligned} g_i &= \mathbb{E} \left[h(\{\mathbf{X}_t^{(i)}\}_{i=1}^m, \{\mathbf{X}_1^{(i)}\}_{i=1}^m) \right. \\ &\quad \left. - \left\| \frac{1}{m} \left(\sum_{j=1, j \neq i}^m \mathbf{f}(\mathbf{X}_t^{(j)}) \mathcal{K}_t(\mathbf{X}_t, \mathbf{X}_1^{(j)}) - \nabla \log p_t(\mathbf{X}_t) \right) \right\|_{L^2(P_{\mathbf{X}_t})} \mid \mathcal{F}_i \right]. \end{aligned}$$

We have

$$h_i = g_i - \mathbb{E}[g_i \mid \mathcal{F}_{i-1}],$$

and

$$\begin{aligned} \mathbb{E}[h_i^k \mid \mathcal{F}_{i-1}] &\leq \mathbb{E}[g_i^k \mid \mathcal{F}_{i-1}] \\ &\leq \frac{1}{m} \mathbb{E} \left[\left[\left\| \mathbf{f}(\mathbf{X}_t^{(i)}) \mathcal{K}_t(\mathbf{X}_t, \mathbf{X}_1^{(i)}) - \nabla \log p_t(\mathbf{X}_t) \right\|_{L^2(P_{\mathbf{X}_t})} \right]^k \mid \mathcal{F}_i \right] \\ &\leq \frac{1}{m} \mathbb{E} \left[\left\| \mathbf{f}(\mathbf{X}_t^{(i)}) \mathcal{K}_t(\mathbf{X}_t, \mathbf{X}_1^{(i)}) - \nabla \log p_t(\mathbf{X}_t) \right\|_{L^2(P_{\mathbf{X}_t})}^k \right] \\ &\leq \frac{k! \sigma_0^2 H_0^{k-2}}{2m^k}. \end{aligned}$$

due to the property of conditional expectation, Jensen's inequality, and Assumption 4. Then, by invoking the above inequality, and relationship $x \leq e^{x-1}$, we have

$$\begin{aligned} \mathbb{E}[\exp(\lambda h_i) \mid \mathcal{F}_{i-1}] &\leq \exp(\mathbb{E}[\exp(\lambda h_i) \mid \mathcal{F}_{i-1}] - 1) \\ &= \exp \left(\mathbb{E} \left[\sum_{k=2}^{\infty} \frac{h_i^k \lambda^k}{k!} \mid \mathcal{F}_{i-1} \right] \right) \\ &\leq \exp \left(\frac{\sigma^2}{2H_0^2} \sum_{k=2}^{\infty} \left(\frac{\lambda H_0}{m} \right)^k \right) \\ &\leq \exp \left(\frac{\lambda^2 \sigma_0^2}{2m^2 \left(1 - \frac{\lambda H_0}{m} \right)} \right), \end{aligned}$$

by taking $0 < \lambda < \frac{m}{H}$. Due to this inequality, we notice

$$\begin{aligned} &\mathbb{E} \left[\exp \left(\lambda (h(\{\mathbf{X}_t^{(i)}\}_{i=1}^m, \{\mathbf{X}_1^{(i)}\}_{i=1}^m) - \mathbb{E}_{\{\mathbf{X}_t^{(i)}\}_{i=1}^m, \{\mathbf{X}_1^{(i)}\}_{i=1}^m} [h(\{\mathbf{X}_t^{(i)}\}_{i=1}^m, \{\mathbf{X}_1^{(i)}\}_{i=1}^m)]) \right) \right] \\ &= \mathbb{E} \left[\exp \left(\lambda \sum_{i=1}^n h_i \right) \right] \\ &= \mathbb{E} \left[\mathbb{E} \left[\exp \left(\lambda \sum_{i=1}^n h_i \right) \mid \mathcal{F}_{n-1} \right] \right] \\ &= \mathbb{E} \left[\mathbb{E} \left[\exp \left(\lambda \sum_{i=1}^{n-1} h_i \right) \mid \mathcal{F}_{n-1} \right] \mathbb{E}[\exp(\lambda h_n) \mid \mathcal{F}_{n-1}] \right] \\ &= \mathbb{E} \left[\prod_{k=1}^m \mathbb{E}[\exp(\lambda h_i) \mid \mathcal{F}_{i-1}] \right] \\ &\leq \mathbb{E} \left[\exp \left(\frac{\lambda^2 \sigma_0^2}{2m \left(1 - \frac{\lambda H_0}{m} \right)} \right) \right]. \end{aligned}$$

Then, by applying Chebyshev's inequality, we know that

$$\begin{aligned}
& \mathbb{P} \left(\left| h(\{\mathbf{X}_t^{(i)}\}_{i=1}^m, \{\mathbf{X}_1^{(i)}\}_{i=1}^m) - \mathbb{E}_{\{\mathbf{X}_t^{(i)}\}_{i=1}^m, \{\mathbf{X}_1^{(i)}\}_{i=1}^m} \left[h(\{\mathbf{X}_t^{(i)}\}_{i=1}^m, \{\mathbf{X}_1^{(i)}\}_{i=1}^m) \right] \right| \geq \delta \right) \\
& \leq 2\mathbb{E} \left[\exp \left(\lambda \left(h(\{\mathbf{X}_t^{(i)}\}_{i=1}^m, \{\mathbf{X}_1^{(i)}\}_{i=1}^m) - \mathbb{E}_{\{\mathbf{X}_t^{(i)}\}_{i=1}^m, \{\mathbf{X}_1^{(i)}\}_{i=1}^m} \left[h(\{\mathbf{X}_t^{(i)}\}_{i=1}^m, \{\mathbf{X}_1^{(i)}\}_{i=1}^m) \right] \right) - \lambda\delta \right) \right] \\
& \leq 2 \exp \left(\frac{\lambda^2 \sigma_0^2}{2m(1 - \frac{\lambda H_0}{m})} - \lambda\delta \right) \\
& = 2 \exp \left(-\frac{m\delta^2}{2(\sigma_0^2 + H_0\delta)} \right).
\end{aligned}$$

by taking $\lambda = \frac{m\delta}{\sigma_0^2 + H_0\delta}$. Moreover, by noting that

$$\begin{aligned}
h(\{\mathbf{X}_t^{(i)}\}_{i=1}^m, \{\mathbf{X}_1^{(i)}\}_{i=1}^m)^2 & \leq \left(\mathbb{E}_{\{\mathbf{X}_t^{(i)}\}_{i=1}^m, \{\mathbf{X}_1^{(i)}\}_{i=1}^m} \left[h(\{\mathbf{X}_t^{(i)}\}_{i=1}^m, \{\mathbf{X}_1^{(i)}\}_{i=1}^m) \right] + \delta \right)^2 \\
& \leq 2\mathbb{E}_{\{\mathbf{X}_t^{(i)}\}_{i=1}^m, \{\mathbf{X}_1^{(i)}\}_{i=1}^m} \left[h(\{\mathbf{X}_t^{(i)}\}_{i=1}^m, \{\mathbf{X}_1^{(i)}\}_{i=1}^m) \right]^2 + 2\delta^2 \\
& \leq 2\mathbb{E}_{\{\mathbf{X}_t^{(i)}\}_{i=1}^m, \{\mathbf{X}_1^{(i)}\}_{i=1}^m} \left[h(\{\mathbf{X}_t^{(i)}\}_{i=1}^m, \{\mathbf{X}_1^{(i)}\}_{i=1}^m) \right]^2 + 2\delta^2 \\
& \leq \frac{2\sigma_0^2}{m} + 2\delta^2,
\end{aligned}$$

the conclusion is proved by taking

$$\delta = \frac{2H_0 \log \left(\frac{2}{\eta} \right) + \sqrt{4H_0^2 \log^2 \left(\frac{2}{\eta} \right) + 8m\sigma_0^2 \log^2 \left(\frac{2}{\eta} \right)}}{2m} \leq \delta_{0m}(\eta),$$

which leads to $2 \exp [-m\delta^2 / \{2(\sigma_0^2 + H_0\delta)\}] = \eta$. \square

Next, let us give the proof of Proposition 2. Before that, we first present the derivation to (10).

Due to the definition of $\mathcal{K}_t(\mathbf{x}_1, \mathbf{x}_2)$ in (10), then by basic algebra, we know that

$$\begin{aligned}
& \mathcal{K}_t(\mathbf{x}_1, \mathbf{x}_2) \\
& = \int_{\mathbb{R}^d} \left(\frac{1}{2\pi|\boldsymbol{\Sigma}|} \right)^{\frac{d}{2}} \exp \left\{ -(\mathbf{x}_1 - \mathbf{x}_2 - i\sqrt{1-t}\boldsymbol{\xi})^\top \mathbf{H}(\mathbf{x}_1 - \mathbf{x}_2 - i\sqrt{1-t}\boldsymbol{\xi}) - \boldsymbol{\xi}^\top \boldsymbol{\Omega} \boldsymbol{\xi} \right\} d\boldsymbol{\xi} \\
& = \int_{\mathbb{R}^d} \left(\frac{1}{2\pi|\boldsymbol{\Sigma}|} \right)^{\frac{d}{2}} \exp \left\{ -[\boldsymbol{\xi} - i\sqrt{1-t}\boldsymbol{\Omega}_t^{-1}\mathbf{H}(\mathbf{x}_1 - \mathbf{x}_2)]^\top \boldsymbol{\Omega}_t [\boldsymbol{\xi} - i\sqrt{1-t}\boldsymbol{\Omega}_t^{-1}\mathbf{H}(\mathbf{x}_1 - \mathbf{x}_2)] \right\} \\
& \quad \cdot \exp \left\{ -(1-t)(\mathbf{x}_1 - \mathbf{x}_2)^\top \mathbf{H}\boldsymbol{\Omega}_t^{-1}\mathbf{H}(\mathbf{x}_1 - \mathbf{x}_2) - (\mathbf{x}_1 - \mathbf{x}_2)^\top \mathbf{H}(\mathbf{x}_1 - \mathbf{x}_2) \right\} d\boldsymbol{\xi} \\
& = \sqrt{|\boldsymbol{\Omega}_t|^{-1}|\boldsymbol{\Omega}|} \exp \left\{ -(1-t)(\mathbf{x}_1 - \mathbf{x}_2)^\top \mathbf{H}\boldsymbol{\Omega}_t^{-1}\mathbf{H}(\mathbf{x}_1 - \mathbf{x}_2) - (\mathbf{x}_1 - \mathbf{x}_2)^\top \mathbf{H}(\mathbf{x}_1 - \mathbf{x}_2) \right\}.
\end{aligned}$$

Due to the matrix equality $(1-t)\mathbf{H}\boldsymbol{\Omega}_t^{-1}\mathbf{H} + \mathbf{H} = \mathbf{H}_t$, we get the (10). Similar to the derivation of (10), we can prove Proposition 2.

Restatement of Proposition 2. With $\mathbf{s}_t(\mathbf{x}; \boldsymbol{\theta}_t)$ defined in (11), an unbiased estimate for the objective (7) is

$$\text{tr} \left\{ \boldsymbol{\theta}_t^\top \mathbf{K}_t^{(1)} + \boldsymbol{\theta}_t^\top \mathbf{K}_t^{(2)} \boldsymbol{\theta}_t \right\},$$

where $\mathbf{K}_t^{(1)}$ is a $m \times d$ matrix whose (i, l) -th element equals to $2(n-m)^{-1} \sum_{k=m+1}^n \mathcal{K}_t^{(1,l)}(\mathbf{X}_1^{(k)}; \mathbf{X}_1^{(i)})$, $\mathbf{K}_t^{(2)}$ is a $m \times m$ matrix whose (i, j) -th element equals to $(n-m)^{-1} \sum_{k=m+1}^n \mathcal{K}_t^{(2)}(\mathbf{X}_1^{(k)}; \mathbf{X}_1^{(i)}, \mathbf{X}_1^{(j)})$,

$$\mathcal{K}_t^{(1,l)}(\mathbf{x}; \mathbf{x}_1) = -2 \frac{|\boldsymbol{\Omega}|}{\sqrt{|\boldsymbol{\Omega}_t| |\boldsymbol{\Omega}_t^{(1)}|}} \mathbf{e}_l^\top \mathbf{H}_t^{(1)}(\mathbf{x} - \mathbf{x}_1) \exp \left\{ -(\mathbf{x} - \mathbf{x}_1)^\top \mathbf{H}_t^{(1)}(\mathbf{x} - \mathbf{x}_1) \right\},$$

and

$$\begin{aligned} \mathcal{K}_t^{(2)}(\mathbf{x}; \mathbf{x}_1, \mathbf{x}_2) &= \frac{|\boldsymbol{\Omega}|^{\frac{3}{2}}}{|\boldsymbol{\Omega}_t| |\boldsymbol{\Omega}_t^{(2)}|^{\frac{1}{2}}} \exp \left\{ -(\mathbf{x}_1 + \mathbf{x}_2 - 2\mathbf{x})^\top \mathbf{H}_t^{(2)}(\mathbf{x}_1 + \mathbf{x}_2 - 2\mathbf{x}) \right\} \\ &\quad \times \exp \left\{ -(\mathbf{x}_1 - \mathbf{x})^\top \mathbf{H}_t(\mathbf{x}_1 - \mathbf{x}) \right\} \\ &\quad \times \exp \left\{ -(\mathbf{x}_2 - \mathbf{x})^\top \mathbf{H}_t(\mathbf{x}_2 - \mathbf{x}) \right\}, \end{aligned}$$

for any \mathbf{x} , \mathbf{x}_1 and \mathbf{x}_2 . Here \mathbf{e}_l is the l -th basis vector in the d -dimensional space, $\boldsymbol{\Omega}_t^{(1)} = \boldsymbol{\Omega} - (1-t)\mathbf{H}_t$, $\mathbf{H}_t^{(1)} = (1-t)\mathbf{H}_t \boldsymbol{\Omega}_t^{(1)-1} \mathbf{H}_t + \mathbf{H}_t$, $\boldsymbol{\Omega}_t^{(2)} = \boldsymbol{\Omega} - 2(1-t)\mathbf{H}_t$ and $\mathbf{H}_t^{(2)} = (1-t)\mathbf{H}_t \boldsymbol{\Omega}_t^{(2)-1} \mathbf{H}_t$.

Proof. According to the formulation (7), it suffices to find the unbiased estimates for

$$\mathbb{E} \left[\left\| \mathbf{s}_t(\mathbf{X}_1 + i\sqrt{1-t}\boldsymbol{\xi}; \boldsymbol{\theta}_t) \right\|^2 \right] \quad \text{and} \quad \mathbb{E} \left[\left\| \mathbf{s}_t(\mathbf{X}_1 + i\sqrt{1-t}\boldsymbol{\xi}; \boldsymbol{\theta}_t) \right\|^2 \right].$$

We first compute

$$\begin{aligned} \mathbb{E} \left[\left\| \mathbf{s}_t(\mathbf{X}_1 + i\sqrt{1-t}\boldsymbol{\xi}; \boldsymbol{\theta}_t) \right\|^2 \right] &= \sum_{l=1}^d \boldsymbol{\theta}_{t,l}^\top \mathbb{E} \left[\mathcal{K}_t(\mathbf{X}_1 + i\sqrt{1-t}\boldsymbol{\xi}; \mathcal{D}_m) \mathcal{K}_t(\mathbf{X}_1 + i\sqrt{1-t}\boldsymbol{\xi}; \mathcal{D}_m)^\top \right] \boldsymbol{\theta}_{t,l} \\ &= \text{tr} \left\{ \boldsymbol{\theta}_t^\top \mathbb{E} \left[\mathcal{K}_t(\mathbf{X}_1 + i\sqrt{1-t}\boldsymbol{\xi}; \mathcal{D}_m) \mathcal{K}_t(\mathbf{X}_1 + i\sqrt{1-t}\boldsymbol{\xi}; \mathcal{D}_m)^\top \right] \boldsymbol{\theta}_t \right\}, \end{aligned}$$

where $\mathcal{D}_m = \{\mathbf{X}_1^{(i)}\}_{i=1}^m$ and $\mathcal{K}_t(\mathbf{x}; \mathcal{D}_m)$ is the vector $(\mathcal{K}_t(\mathbf{x}, \mathbf{X}_1^{(1)}), \dots, \mathcal{K}_t(\mathbf{x}, \mathbf{X}_1^{(m)}))^\top$. Some tedious calculations can show that

$$\mathbb{E}[\mathcal{K}_t(\mathbf{X}_1 + i\sqrt{1-t}\boldsymbol{\xi}, \mathbf{X}_1^{(i)}) \mathcal{K}_t(\mathbf{X}_1 + i\sqrt{1-t}\boldsymbol{\xi}, \mathbf{X}_1^{(j)})] = E_{\mathbf{X}_1}[\mathcal{K}_t^{(2)}(\mathbf{X}_1; \mathbf{X}_1^{(i)}, \mathbf{X}_1^{(j)})],$$

for $1 \leq i, j \leq m$, which can be unbiasedly estimated by $(n-m)^{-1} \sum_{k=m+1}^n \mathcal{K}_t^{(2)}(\mathbf{X}_1^{(k)}; \mathbf{X}_1^{(i)}, \mathbf{X}_1^{(j)})$.

Furthermore, we have

$$2\text{tr} \left\{ \mathbb{E} \left[\nabla \mathbf{s}_t(\mathbf{X}_1 + i\sqrt{1-t}\boldsymbol{\xi}; \boldsymbol{\theta}_t) \right] \right\} = 2\text{tr} \left[\boldsymbol{\theta}_t^\top \mathbb{E} \left\{ \nabla \mathcal{K}_t(\mathbf{X}_1; \mathcal{D}_m) \right\} \right].$$

Straightforward calculations can show that

$$2\mathbb{E} \left[\frac{\partial}{\partial x_l} \mathcal{K}_t(\mathbf{X}_1 + i\sqrt{1-t}\boldsymbol{\xi}; \mathbf{X}_1^{(i)}) \right] = \mathbb{E} \left[\mathcal{K}_t^{(1,l)}(\mathbf{X}_1, \mathbf{X}_1^{(i)}) \right],$$

which can be unbiasedly estimated by

$$2(n-m)^{-1} \sum_{k=m+1}^n \mathcal{K}_t^{(1,l)}(\mathbf{X}_1^{(k)}; \mathbf{X}_1^{(i)}).$$

This completes the proof. \square

E Proofs for Results in Section 4.1

In this section, we will prove one of our main Theorem 1, our proof is developed on the method proposed in (Lee et al., 2022; Chen et al., 2022, 2023). To do so, we need several lemmas. Firstly, we rewrite the sampling process of data $\widehat{\mathbf{X}}_t$ as the following SDE

$$\begin{cases} d\widehat{\mathbf{X}}_t = \boldsymbol{\Sigma} \mathbf{s}_{1-k/K} \left(\widehat{\mathbf{X}}_{k/K}; \widehat{\boldsymbol{\theta}}_{1-k/K} \right) dt + \boldsymbol{\Sigma}^{\frac{1}{2}} dW_t; & \frac{k}{K} \leq t < \frac{k+1}{K}; \\ P_{\widehat{\mathbf{X}}_0} = P_{\mathbf{X}_1}, k = 1, \dots, K-1. \end{cases} \quad (19)$$

By involving such SDE, we can upper bound the gap between $P_{\widehat{\mathbf{X}}_1}$ and the desired $P_{\mathbf{X}_0} = P_{\widetilde{\mathbf{X}}_1}$ by applying Girsanov's theorem (Oksendal, 2013). To simplify the notation, we define

$$\widehat{\mathbf{s}}_t(\mathbf{X}_t) = \mathbf{s}_{1-k/K} \left(\mathbf{X}_{k/K}; \widehat{\boldsymbol{\theta}}_{1-k/K} \right); \quad \frac{k}{K} \leq t < \frac{k+1}{K},$$

for any given SDE \mathbf{X}_t . Based on these notations, we have the following lemma, which is a direct consequence of Girsanov's theorem (Oksendal, 2013), where the imposed Novikov's condition (20) has been discussed in Section B.

Lemma 2 (Girsanov's Theorem). *Let $P_{\widetilde{\mathbf{X}}_{[0,1]}}$ and $P_{\widehat{\mathbf{X}}_{[0,1]}}$ respectively be the probability measures on the path space $\mathcal{C}([0, 1]; \mathbb{R}^d)$ of SDE (5) and (19). Then, if the Novikov's condition imposed in Section B*

$$\mathbb{E}_{\widetilde{\mathbf{X}}_t} \left[\frac{1}{2} \int_0^1 \exp \left(\left\| \boldsymbol{\Sigma}^{\frac{1}{2}} \left(\nabla_{\mathbf{x}} \log p_{1-t}(\widetilde{\mathbf{X}}_t) - \widehat{\mathbf{s}}_t(\widetilde{\mathbf{X}}_t) \right) \right\|^2 \right) dt \right] < \infty \quad (20)$$

is satisfied, we have that

$$\begin{aligned} \frac{dP_{\widetilde{\mathbf{X}}_{[0,1]}}}{dP_{\widetilde{\mathbf{X}}_{[0,1]}}} &= \exp \left\{ - \int_0^1 \boldsymbol{\Sigma}^{\frac{1}{2}} \left(\nabla_{\mathbf{x}} \log p_{1-t}(\widetilde{\mathbf{X}}_t) - \hat{\mathbf{s}}_t(\widetilde{\mathbf{X}}_t) \right) dW_t \right. \\ &\quad \left. - \frac{1}{2} \int_0^1 \left\| \boldsymbol{\Sigma}^{\frac{1}{2}} \left(\nabla_{\mathbf{x}} \log p_{1-t}(\widetilde{\mathbf{X}}_t) - \hat{\mathbf{s}}_t(\widetilde{\mathbf{X}}_t) \right) \right\|^2 dt \right\}, \end{aligned}$$

where W_t is Brownian motion under $P_{\widetilde{\mathbf{X}}_{[0,1]}}$.

By applying this lemma, we have the following conclusion as a direct consequence.

Lemma 3. *If the Novikov's condition (20) is satisfied, then*

$$D_{KL} \left(P_{\widetilde{\mathbf{X}}_1} \parallel P_{\widehat{\mathbf{X}}_1} \right) \leq \mathbb{E}_{\widetilde{\mathbf{X}}_t} \left[\int_0^1 (1-t) \lambda_{\max}(\boldsymbol{\Sigma}) \left\| \nabla_{\mathbf{x}} \log p_{1-t}(\widetilde{\mathbf{X}}_t) - \hat{\mathbf{s}}_t(\widetilde{\mathbf{X}}_t) \right\|^2 \right].$$

Proof. According to the data-processing inequality of KL-divergence (Cover, 1999), we have

$$\begin{aligned} D_{KL} \left(P_{\widetilde{\mathbf{X}}_1} \parallel P_{\widehat{\mathbf{X}}_1} \right) &\leq D_{KL} \left(P_{\widetilde{\mathbf{X}}_{[0,1]}} \parallel P_{\widehat{\mathbf{X}}_{[0,1]}} \right) \\ &= \int \log \frac{dP_{\widetilde{\mathbf{X}}_{[0,1]}}}{dP_{\widehat{\mathbf{X}}_{[0,1]}}} dP_{\widetilde{\mathbf{X}}_{[0,1]}} \\ &= \mathbb{E}_{\widetilde{\mathbf{X}}_t} \left[\frac{1}{2} \int_0^1 \left\| \boldsymbol{\Sigma}^{\frac{1}{2}} \left(\nabla_{\mathbf{x}} \log p_{1-t}(\widetilde{\mathbf{X}}_t) - \hat{\mathbf{s}}_t(\widetilde{\mathbf{X}}_t) \right) \right\|^2 dt \right] \\ &\leq \mathbb{E}_{\widetilde{\mathbf{X}}_t} \left[\frac{1}{2} \int_0^1 \left\| \boldsymbol{\Sigma}^{\frac{1}{2}} \left(\nabla_{\mathbf{x}} \log p_{1-t}(\widetilde{\mathbf{X}}_t) - \hat{\mathbf{s}}_t(\widetilde{\mathbf{X}}_t) \right) \right\|^2 dt \right] \\ &\leq \frac{1}{2} \mathbb{E}_{\widetilde{\mathbf{X}}_t} \left[\int_0^1 \lambda_{\max}(\boldsymbol{\Sigma}) \left\| \nabla_{\mathbf{x}} \log p_{1-t}(\widetilde{\mathbf{X}}_t) - \hat{\mathbf{s}}_t(\widetilde{\mathbf{X}}_t) \right\|^2 \right], \end{aligned}$$

where the second equality is due to Lemma 2, and the property of Itô integral (Oksendal, 2013). \square

The lemma indicates that the gap between the distributions of sampled data $P_{\widetilde{\mathbf{X}}_1}$ and the desired ground truth $P_{\mathbf{X}_1}$ is decided by the difference between our model $\mathbf{s}(\mathbf{x}; \widehat{\boldsymbol{\theta}}_t)$ and the ground truth score function. Next, let us characterize such a difference.

To do so, by simple algebra, we have

$$\begin{aligned}
& \mathbb{E}_{\widetilde{\mathbf{X}}_t} \left[\int_0^1 \lambda_{\max}(\boldsymbol{\Sigma}) \left\| \nabla_{\mathbf{x}} \log p_{1-t}(\widetilde{\mathbf{X}}_t) - \hat{\mathbf{s}}_t(\widetilde{\mathbf{X}}_t, \widehat{\boldsymbol{\theta}}_{1-t}) \right\|^2 \right] \\
&= \sum_{k=0}^{K-1} \mathbb{E}_{\widetilde{\mathbf{X}}_t} \left[\int_{\frac{k}{K}}^{\frac{k+1}{K}} \lambda_{\max}(\boldsymbol{\Sigma}) \left\| \nabla_{\mathbf{x}} \log p_{1-t}(\widetilde{\mathbf{X}}_t) - \hat{\mathbf{s}}_t(\widetilde{\mathbf{X}}_t, \widehat{\boldsymbol{\theta}}_{1-t}) \right\|^2 \right] \\
&\leq 4 \sum_{k=0}^{K-1} \mathbb{E}_{\widetilde{\mathbf{X}}_t} \left[\int_{\frac{k}{K}}^{\frac{k+1}{K}} \lambda_{\max}(\boldsymbol{\Sigma}) \left\| \nabla_{\mathbf{x}} \log p_{1-t}(\widetilde{\mathbf{X}}_t) - \nabla_{\mathbf{x}} \log p_{1-t}(\widetilde{\mathbf{X}}_{k/K}) \right\|^2 \right] \\
&+ 4 \sum_{k=0}^{K-1} \mathbb{E}_{\widetilde{\mathbf{X}}_t} \left[\int_{\frac{k}{K}}^{\frac{k+1}{K}} \lambda_{\max}(\boldsymbol{\Sigma}) \left\| \nabla_{\mathbf{x}} \log p_{1-t}(\widetilde{\mathbf{X}}_{k/K}) - \nabla_{\mathbf{x}} \log p_{1-k/K}(\widetilde{\mathbf{X}}_{k/K}) \right\|^2 \right] \\
&+ 4 \sum_{k=0}^{K-1} \mathbb{E}_{\widetilde{\mathbf{X}}_t} \left[\int_{\frac{k}{K}}^{\frac{k+1}{K}} \lambda_{\max}(\boldsymbol{\Sigma}) \left\| \hat{\mathbf{s}}(\widetilde{\mathbf{X}}_{k/K}, \boldsymbol{\theta}_{1-k/K}) - \nabla_{\mathbf{x}} \log p_{1-k/K}(\widetilde{\mathbf{X}}_{k/K}) \right\|^2 \right].
\end{aligned} \tag{21}$$

Next, we respectively upper bound the three terms in the above inequality to characterize the final sampling error. First, we use the Lipschitz continuity assumption 3 to upper bounded the first term.

Lemma 4. For $\widetilde{\mathbf{X}}_t$ follows (5), and $k/K \leq t < (k+1)/K$, we have

$$\mathbb{E} \left[\left\| \nabla_{\mathbf{x}} \log p_{1-t}(\widetilde{\mathbf{X}}_t) - \nabla_{\mathbf{x}} \log p_{1-t}(\widetilde{\mathbf{X}}_{k/K}) \right\|^2 \right] \leq \frac{2L\text{tr}\{\boldsymbol{\Sigma}\}}{K} + \frac{2L_{\mathbf{x}}^2 d \lambda_{\max}(\boldsymbol{\Sigma})}{K^2}$$

Proof. Due to the Lipschitz continuity assumption 3, we have

$$\begin{aligned}
& \mathbb{E}_{\widetilde{\mathbf{X}}_t} \left[\left\| \nabla_{\mathbf{x}} \log p_{1-t}(\widetilde{\mathbf{X}}_t) - \nabla_{\mathbf{x}} \log p_{1-t}(\widetilde{\mathbf{X}}_{k/K}) \right\|^2 \right] \leq L \mathbb{E} \left[\left\| \widetilde{\mathbf{X}}_t - \widetilde{\mathbf{X}}_{k/K} \right\|^2 \right] \\
&\leq 2L \mathbb{E} \left[\left\| \int_{\frac{k}{K}}^t \boldsymbol{\Sigma} \nabla_{\mathbf{x}} \log p_{1-s}(\widetilde{\mathbf{X}}_s) ds \right\|^2 + \left\| \int_{\frac{k}{K}}^t \boldsymbol{\Sigma}^{\frac{1}{2}} dW_s \right\|^2 \right].
\end{aligned} \tag{22}$$

Then we have

$$\mathbb{E} \left[\left\| \int_{\frac{k}{K}}^t \boldsymbol{\Sigma}^{\frac{1}{2}} dW_s \right\|^2 \right] = \text{tr}\{\boldsymbol{\Sigma}\} \int_{\frac{k}{K}}^t ds = \text{tr}\{\boldsymbol{\Sigma}\} \left(t - \frac{k}{K} \right). \tag{23}$$

On the other hand, by Schwarz's inequality

$$\mathbb{E} \left[\left\| \int_{\frac{k}{K}}^t \boldsymbol{\Sigma} \nabla_{\mathbf{x}} \log p_{1-s}(\widetilde{\mathbf{X}}_s) ds \right\|^2 \right] \leq \lambda_{\max}^2(\boldsymbol{\Sigma}) \left(t - \frac{k}{K} \right) \mathbb{E} \left[\int_{\frac{k}{K}}^t \left\| \nabla_{\mathbf{x}} \log p_{1-s}(\widetilde{\mathbf{X}}_s) \right\|^2 ds \right]. \tag{24}$$

By taking integral by part,

$$\begin{aligned}
\mathbb{E} \left[\left\| \nabla_{\mathbf{x}} \log p_{1-s}(\widetilde{\mathbf{X}}_s) \right\|^2 \right] &= \int_{\mathbb{R}^d} p_{1-s}(\mathbf{x}) \nabla_{\mathbf{x}} \log p_{1-s}(\mathbf{x})^\top \nabla_{\mathbf{x}} \log p_{1-s}(\mathbf{x}) d\mathbf{x} \\
&= - \int_{\mathbb{R}^d} p_{1-s}(\mathbf{x}) \text{tr}\{\nabla_{\mathbf{x}}^2 \log p_{1-s}(\mathbf{x})\} d\mathbf{x} \\
&\leq Ld,
\end{aligned} \tag{25}$$

where the last inequality is due to the Lipschitz continuity assumption 3. Plugging this into (24) and combining it with (23) and (22), we get the conclusion. \square

Then we proceed to use the following lemma to upper bound the second term in the R.H.S. of inequality (21). The result is similar to the Lemma 1 in (Chen et al., 2023) and Lemma C.12 in (Lee et al., 2022)

Lemma 5. *Let $\widetilde{\mathbf{X}}_t$ follows (5), $K^2 \geq 4\lambda_{\max}(\boldsymbol{\Sigma})L$ and $k/K \leq t < (k+1)/K$, then we have*

$$\mathbb{E} \left[\left\| \nabla_{\mathbf{x}} \log p_{1-t} \left(\widetilde{\mathbf{X}}_{k/K} \right) - \nabla_{\mathbf{x}} \log p_{1-k/K} \left(\widetilde{\mathbf{X}}_{k/K} \right) \right\|^2 \right] \leq \frac{6dL^2\lambda_{\max}(\boldsymbol{\Sigma})}{K^2}$$

Proof. Let $V_0(\mathbf{x})$ denote $\log p_0(\mathbf{x})$ ⁶, then for any t , we have

$$\begin{aligned} \log p_t(\mathbf{x}) &= \log \int_{\mathbb{R}^d} p_{t|0}(\mathbf{x} | \mathbf{x}_0) p_0(\mathbf{x}_0) d\mathbf{x}_0 \\ &\propto \log \int_{\mathbb{R}^d} \exp(\log p_{t|0}(\mathbf{x} | \mathbf{x}_0) + V_0(\mathbf{x}_0)) d\mathbf{x}_0 \\ &= \log \int_{\mathbb{R}^d} \exp\left(-\frac{1}{2t^2}(\mathbf{x}_0 - \mathbf{x})^\top \boldsymbol{\Sigma}^{-1}(\mathbf{x}_0 - \mathbf{x}) + V_0(\mathbf{x}_0)\right) d\mathbf{x}_0 \\ &= \log \int_{\mathbb{R}^d} \exp\left(-\frac{1}{2t^2}\mathbf{x}_0^\top \boldsymbol{\Sigma}^{-1}\mathbf{x}_0 + V_0(\mathbf{x}_0 - \mathbf{x})\right) d\mathbf{x}_0 \end{aligned}$$

Taking gradient w.r.t. \mathbf{x} to the two sides of the equality, and due to the formula of (4), we get

$$\begin{aligned} \nabla \log p_t(\mathbf{x}) &= \frac{\int_{\mathbb{R}^d} -\exp\left(-\frac{1}{2t^2}\mathbf{x}_0^\top \boldsymbol{\Sigma}^{-1}\mathbf{x}_0 + V_0(\mathbf{x}_0 - \mathbf{x})\right) \nabla_{\mathbf{x}} V_0(\mathbf{x}_0 - \mathbf{x}) d\mathbf{x}_0}{\int_{\mathbb{R}^d} \exp\left(-\frac{1}{2t^2}\mathbf{x}_0^\top \boldsymbol{\Sigma}^{-1}\mathbf{x}_0 + V_0(\mathbf{x}_0 - \mathbf{x})\right) d\mathbf{x}_0} \\ &= \int_{\mathbb{R}^d} \frac{p_{t|0}(\mathbf{x} | \mathbf{x}_0) P_0(\mathbf{x}_0)}{P_t(\mathbf{x})} \nabla_{\mathbf{x}} V_0(\mathbf{x}_0) d\mathbf{x}_0 \\ &= \mathbb{E}_{\mathbf{X}_0 | \mathbf{X}_t = \mathbf{x}} [\nabla_{\mathbf{x}} V_0(\mathbf{X}_0)]. \end{aligned}$$

Thus, for any \mathbf{x} , we have

$$\begin{aligned} \left\| \nabla_{\mathbf{x}} \log p_{1-t}(\mathbf{x}) - \nabla_{\mathbf{x}} \log p_{1-k/K}(\mathbf{x}) \right\|^2 &= \left\| \mathbb{E}_{\mathbf{X}_0 | \mathbf{X}_{1-t} = \mathbf{x}} [\nabla_{\mathbf{x}} V_0(\mathbf{X}_0)] - \mathbb{E}_{\mathbf{X}_0 | \mathbf{X}_{1-k/K} = \mathbf{x}} [\nabla_{\mathbf{x}} V_0(\mathbf{X}_0)] \right\|^2 \\ &\leq L^2 \mathbb{W}_1^2 \left(P_{\mathbf{X}_0 | \mathbf{X}_{1-t} = \mathbf{x}}, P_{\mathbf{X}_0 | \mathbf{X}_{1-k/K} = \mathbf{x}} \right), \end{aligned} \tag{26}$$

where the inequality is because $\nabla_{\mathbf{x}} V_0(\mathbf{x})$ is L -continuous and the definition of the first-order Wasserstein distance. As can be seen, obtaining the above results only relies on the Lipschitz

⁶ $p_{t|0}(\cdot | \cdot)$ is the conditional density of $P_{\mathbf{X}_t | \mathbf{X}_0}$

continuity of $\nabla_{\mathbf{x}} V_0(\mathbf{x})$ in Assumption 3. Thus, the $\nabla \log p_t(\mathbf{x}) = \mathbb{E}_{\mathbf{X}_0|\mathbf{X}_t=\mathbf{x}}[\mathbf{X}_0]$ can be substituted with $\nabla \log p_t(\mathbf{x}) = \mathbb{E}_{\mathbf{X}_s|\mathbf{X}_t=\mathbf{x}}[\mathbf{X}_s]$ for any $0 \leq s < t$. Thus, without loss of generality, we can take $k = K - 1$, $0 \leq 1 - t < 1/K$ and the following analysis can be generalized to any other t . Note that

$$P_{\mathbf{X}_0|\mathbf{X}_{1/K}=\mathbf{x}} \propto \exp\left(-\frac{K^2}{2}(\mathbf{X}_0 - \mathbf{x})^\top \Sigma^{-1}(\mathbf{X}_0 - \mathbf{x}) + V_0(\mathbf{x})\right).$$

Since $\lambda_{\max} \nabla^2(V_0(\mathbf{x})) \leq L$, and $K^2 \geq 4\lambda_{\max}(\Sigma)L$, then the conditional density $P_{\mathbf{X}_0|\mathbf{X}_{1/K}=\mathbf{x}}$ is $\frac{K^2}{4\lambda_{\max}(\Sigma)}$ -strongly log-concave. Then by Talagrand's transport cost inequality (Wainwright, 2019), we have

$$W_1^2\left(P_{\mathbf{X}_0|\mathbf{X}_{1-t}=\mathbf{x}}, P_{\mathbf{X}_0|\mathbf{X}_{k/K}=\mathbf{x}}\right) \leq \frac{4\lambda_{\max}(\Sigma)}{K^2} D_{KL}\left(P_{\mathbf{X}_0|\mathbf{X}_{1-t}=\mathbf{x}} \parallel P_{\mathbf{X}_0|\mathbf{X}_{1/K}=\mathbf{x}}\right). \quad (27)$$

Taking expectation to \mathbf{x} with $\mathbf{x} = \mathbf{X}_{1/K}$, due to the convexity of we get

$$\begin{aligned} \mathbb{E}_{\mathbf{x} \sim \mathbf{X}_{1-t}} \left[D_{KL}\left(P_{\mathbf{X}_0|\mathbf{X}_{1-t}=\mathbf{x}} \parallel P_{\mathbf{X}_0|\mathbf{X}_{1/K}=\mathbf{x}}\right) \right] &= D_{KL}\left(P_{\mathbf{X}_0|\mathbf{X}_{1-t}} \parallel P_{\mathbf{X}_0|\mathbf{X}_{1/K}}\right) - D_{KL}\left(P_{\mathbf{X}_{1-t}} \parallel P_{\mathbf{X}_0}\right) \\ &\leq D_{KL}\left(P_{\mathbf{X}_0|\mathbf{X}_{1-t}} \parallel P_{\mathbf{X}_0|\mathbf{X}_{1/K}}\right), \end{aligned}$$

where we use the chain rule of conditional KL divergence.

$$\begin{aligned} D_{KL}\left(P_{\mathbf{X}_0|\mathbf{X}_{1-t}} \parallel P_{\mathbf{X}_0|\mathbf{X}_{1-k/K}}\right) &= \mathbb{E}_{\mathbf{x}_0} \left[D_{KL}\left(P_{\mathbf{X}_{1-t}|\mathbf{x}_0} \parallel P_{\mathbf{X}_{k/K}|\mathbf{x}_0}\right) \right] \\ &= \mathbb{E} \left[D_{KL}\left(\mathcal{N}(\mathbf{x}_0, (1-t)^2 \Sigma) \parallel \mathcal{N}\left(\mathbf{x}_0, \frac{1}{K^2} \Sigma\right)\right) \right] \\ &= \frac{1}{2} \left[\log \left(\frac{1}{(1-t)^2 K^2} \right)^{\frac{d}{2}} - d + \text{tr} \{ K^2 (1-t)^2 \mathbf{I} \} \right] \\ &\leq \frac{3d}{2}, \end{aligned}$$

where the last inequality is due to the value of $1 - t$. Then combining this with (26) and (27), we get the conclusion. \square

With all these lemmas, we are ready to prove Theorem 1.

Restatement of Theorem 1. Suppose the $\widehat{\mathbf{X}}_0 \sim P_{\mathbf{X}_1}$ is independent of $\widehat{\boldsymbol{\theta}}_t$, and $\widehat{\mathbf{X}}_1$ is generated based on the initial point $\widehat{\mathbf{X}}_0$ following the diffusion updates in (15). Under Assumption 3 in Supplementary Material B.2, and assume that for all $t \in [0, 1]$,

$$\mathbb{E} \left[\left\| \mathbf{s}_t(\mathbf{X}_t; \widehat{\boldsymbol{\theta}}_t) - \nabla \log p_t(\mathbf{X}_t) \right\|^2 \right] \leq \delta.$$

Then,

$$D_{KL} \left(P_{\mathbf{X}_0} \parallel P_{\widehat{\mathbf{X}}_1} \right) \leq \mathcal{O} \left(\frac{\lambda_{\max}(\boldsymbol{\Sigma}) L \text{tr}\{\boldsymbol{\Sigma}\}}{K} + \frac{dL\lambda_{\max}^2(\boldsymbol{\Sigma})}{K^2} + \lambda_{\max}(\boldsymbol{\Sigma})\delta \right).$$

Proof. The theorem is directly obtained by combining (21), Lemmas 4, and 5. As can be seen, since $P_{\widetilde{\mathbf{X}}_t} = P_{\mathbf{X}_{1-t}}$, by plugging Lemmas 4, 5, and condition $\mathbb{E}_{\mathbf{x}_t} [\|\mathbf{s}_\theta(\mathbf{x}_t, t) - \nabla_{\mathbf{x}} \log p_t(\mathbf{x}_t)\|^2] \leq \delta$ into (21), we have

$$\begin{aligned} D_{KL} \left(P_{\widetilde{\mathbf{X}}_1} \parallel P_{\widehat{\mathbf{X}}_1} \right) &\leq 4 \sum_{k=0}^{K-1} \int_{\frac{k}{K}}^{\frac{k+1}{K}} \lambda_{\max}(\boldsymbol{\Sigma}) \left(\frac{2L \text{tr}\{\boldsymbol{\Sigma}\}}{K} + \frac{2L_x^2 d \lambda_{\max}(\boldsymbol{\Sigma})}{K^2} \right) dt \\ &\quad + 4 \sum_{k=0}^{K-1} \int_{\frac{k}{K}}^{\frac{k+1}{K}} \lambda_{\max}(\boldsymbol{\Sigma}) \frac{6dL^2 \lambda_{\max}(\boldsymbol{\Sigma})}{K^2} dt \\ &\quad + 4 \sum_{k=0}^{K-1} \int_{\frac{k}{K}}^{\frac{k+1}{K}} \lambda_{\max}(\boldsymbol{\Sigma}) \delta dt \\ &= \mathcal{O} \left(\frac{\lambda_{\max}(\boldsymbol{\Sigma}) L \text{tr}\{\boldsymbol{\Sigma}\}}{K} + \frac{dL\lambda_{\max}^2(\boldsymbol{\Sigma})}{K^2} + \lambda_{\max}(\boldsymbol{\Sigma})\delta \right), \end{aligned}$$

which completes the proof by noting that $\widetilde{\mathbf{X}}_1 \sim P_{\mathbf{X}_0}$. \square

F Proof for Results in Section 4.2

Restatement of Theorem 2. Suppose $\lambda > 2\delta_{2n}(\eta)$. Under Assumption 1 and Assumption 5 in Supplementary Material B.3, for any $t \in [0, 1]$,

$$\begin{aligned} &\mathbb{E}_{\mathbf{X}_t} \left[\left\| \mathbf{s}_t(\mathbf{X}_t; \widehat{\boldsymbol{\theta}}_t) - \nabla \log p_t(\mathbf{X}_t) \right\|^2 \right] \\ &\leq 2\lambda \mathcal{B}_K \log(\eta^{-1}) + \frac{4\sigma_0^2}{m} + 4\delta_{0m}(\eta)^2 + \frac{4(\delta_{1n}(\eta) + 2\delta_{2n}(\eta)\sqrt{C_{\eta,m,\lambda}})^2}{\lambda} \end{aligned}$$

holds with probability at least $1 - 4\eta$, where the randomness is from that of $\widehat{\boldsymbol{\theta}}_t$.

Proof. Let $\bar{\boldsymbol{\theta}}_t = \frac{1}{m}(\mathbf{f}(\mathbf{X}_t^{(1)}), \dots, \mathbf{f}(\mathbf{X}_t^{(m)}))^\top$ where \mathbf{f} is defined above (9). Then, we have

$$\mathbb{E}_{\mathbf{X}_t} \left[\left\| \mathbf{s}(\mathbf{X}_t; \bar{\boldsymbol{\theta}}_t) - \nabla \log p_t(\mathbf{X}_t) \right\|^2 \right] \leq \frac{2\sigma_0^2}{m} + 2\delta_{0m}(\eta)^2 \quad (28)$$

with probability at least $1 - \eta$ according to the proof of Proposition 1. Let $\widehat{\boldsymbol{\zeta}}_t = (n-m)^{-1} \sum_{i=m+1}^n \boldsymbol{\zeta}_{\mathbf{X}_1^{(i)}, t}$

$\boldsymbol{\zeta}_t = \mathbb{E}[\boldsymbol{\zeta}_{\mathbf{X}_1, t}]$, $\widehat{\boldsymbol{\Gamma}}_t = (n-m)^{-1} \sum_{i=m+1}^n \boldsymbol{\Gamma}_{\mathbf{X}_1^{(i)}, t}$ and $\boldsymbol{\Gamma}_t = \mathbb{E}[\boldsymbol{\Gamma}_{\mathbf{X}_1, t}]$ (see definitions in Appendix

B.3). Under Assumption 5, we have

$$\left\| \widehat{\boldsymbol{\zeta}}_t - \boldsymbol{\zeta}_t \right\|_{\mathcal{H}_K^d} \leq 2 \left(\frac{H_1}{n-m} + \frac{\sigma_1}{\sqrt{n-m}} \right) \log \frac{2}{\eta} = \delta_{1n}(\eta) \quad (29)$$

and

$$\left\| \widehat{\boldsymbol{\Gamma}}_t - \boldsymbol{\Gamma}_t \right\|_{\text{HS}} \leq 2 \left(\frac{H_2}{n-m} + \frac{\sigma_2}{\sqrt{n-m}} \right) \log \frac{2}{\eta} = \delta_{2n}(\eta) \quad (30)$$

with probability at least $1 - 2\eta$ according to Proposition 23 in Bauer et al. (2007) (similar to the proof of our Proposition 1). Subsequently, we write $\mathbf{s}(\cdot, \boldsymbol{\theta}_t)$ as $\mathbf{s}_{\boldsymbol{\theta}_t}$ for simplicity. Notice that the objective function can be written as

$$\widehat{\mathcal{L}}_t(\boldsymbol{\theta}_t) = \left\langle \mathbf{s}_{\boldsymbol{\theta}_t}, (\widehat{\boldsymbol{\Gamma}}_t + \lambda \mathbf{I}) \mathbf{s}_{\boldsymbol{\theta}_t} \right\rangle_{\mathcal{H}_{\mathcal{K}}^d} + \left\langle \widehat{\boldsymbol{\zeta}}_t, \mathbf{s}_{\boldsymbol{\theta}_t} \right\rangle_{\mathcal{H}_{\mathcal{K}}^d},$$

where \mathbf{I} is the identity mapping. Let

$$\mathcal{L}_t(\boldsymbol{\theta}_t) = \langle \mathbf{s}_{\boldsymbol{\theta}_t}, (\boldsymbol{\Gamma}_t + \lambda \mathbf{I}) \mathbf{s}_{\boldsymbol{\theta}_t} \rangle_{\mathcal{H}_{\mathcal{K}}^d} + \langle \boldsymbol{\zeta}_t, \mathbf{s}_{\boldsymbol{\theta}_t} \rangle_{\mathcal{H}_{\mathcal{K}}^d},$$

and $\bar{\boldsymbol{\theta}}_{t,\lambda}$ be the minimizer of $\mathcal{L}_t(\boldsymbol{\theta}_t)$. Then,

$$\mathcal{L}_t(\boldsymbol{\theta}_t) = \mathbb{E}_{\mathbf{X}_t} \left[\|\mathbf{s}(\mathbf{X}_t; \boldsymbol{\theta}_t) - \nabla \log p_t(\mathbf{X}_t)\|^2 \right] + \lambda \|\mathbf{s}_{\boldsymbol{\theta}_t}\|_{\mathcal{H}_{\mathcal{K}}^d}^2.$$

Notice that $\sup_{\mathbf{x}_1, \mathbf{x}_2} \mathcal{K}_t^{(0)}(\mathbf{x}_1, \mathbf{x}_2) \leq |\boldsymbol{\Omega}_t^{(0)}|^{-1/2} |\boldsymbol{\Omega}^{(0)}|^{1/2}$ and $\mathbf{f}_t(\mathbf{x}_1)^\top \mathbf{f}_t(\mathbf{x}_2) \leq 1/2(\|\mathbf{f}_t(\mathbf{x}_1)\|^2 + \|\mathbf{f}_t(\mathbf{x}_2)\|^2)$ for any $\mathbf{x}_1, \mathbf{x}_2 \in \mathbb{R}^d$. We have $\mathbb{E} \left[\exp \left\{ m^{-2} \sum_{i,j=1}^m \mathbf{f}_t(\mathbf{X}_1^{(i)})^\top \mathbf{f}_t(\mathbf{X}_1^{(j)}) \mathcal{K}_t^{(0)}(\mathbf{X}_1^{(i)}, \mathbf{X}_1^{(j)}) \right\} \right] \leq \exp(B_{\mathcal{K}})$ according to Assumption 1 and Jensen's inequality. Then, by Chebyshev's inequality, we have

$$\|\mathbf{s}_{\bar{\boldsymbol{\theta}}_t}\|_{\mathcal{H}_{\mathcal{K}}^d}^2 \leq B_{\mathcal{K}} \log(\eta^{-1}),$$

with probability at least $1 - \eta$. Combining this with (28), we have

$$\begin{aligned} \mathbb{E}_{\mathbf{X}_t} \left[\|\mathbf{s}(\mathbf{X}_t; \bar{\boldsymbol{\theta}}_{t,\lambda}) - \nabla \log p_t(\mathbf{X}_t)\|^2 \right] &\leq \mathbb{E}_{\mathbf{X}_t} \left[\|\mathbf{s}(\mathbf{X}_t; \bar{\boldsymbol{\theta}}_t) - \nabla \log p_t(\mathbf{X}_t)\|^2 \right] + \lambda \|\mathbf{s}_{\bar{\boldsymbol{\theta}}_t}\|_{\mathcal{H}_{\mathcal{K}}^d}^2 \\ &\leq \frac{2\sigma_0^2}{m} + 2\delta_{0m}(\eta)^2 + \lambda B_{\mathcal{K}} \log(\eta^{-1}) \end{aligned} \quad (31)$$

and

$$\begin{aligned} \left\| \mathbf{s}_{\bar{\boldsymbol{\theta}}_{t,\lambda}} \right\|_{\mathcal{H}_{\mathcal{K}}^d}^2 &\leq \lambda^{-1} \mathbb{E}_{\mathbf{X}_t} \left[\|\mathbf{s}(\mathbf{X}_t; \bar{\boldsymbol{\theta}}_t) - \nabla \log p_t(\mathbf{X}_t)\|^2 \right] + \|\mathbf{s}_{\bar{\boldsymbol{\theta}}_t}\|_{\mathcal{H}_{\mathcal{K}}^d}^2 \\ &\leq \lambda^{-1} \left\{ \frac{2\sigma_0^2}{m} + 2\delta_{0m}(\eta)^2 \right\} + B_{\mathcal{K}} \log(\eta^{-1}) \\ &= C_{\eta,m,\lambda} \end{aligned} \quad (32)$$

with probability at least $1 - \eta$ by the definition of $\bar{\boldsymbol{\theta}}_{t,\lambda}$. Next, we bound the gap between $\mathbf{s}_{\hat{\boldsymbol{\theta}}_t}$ and $\mathbf{s}_{\bar{\boldsymbol{\theta}}_{t,\lambda}}$. Recall that $\hat{\boldsymbol{\theta}}_t$ is the minimizer of $\hat{\mathcal{L}}_t(\boldsymbol{\theta}_t)$. Thus,

$$\left\langle \mathbf{s}_{\hat{\boldsymbol{\theta}}_t}, (\hat{\boldsymbol{\Gamma}}_t + \lambda \mathbf{I}) \mathbf{s}_{\hat{\boldsymbol{\theta}}_t} \right\rangle_{\mathcal{H}_{\mathcal{K}}^d} + \left\langle \hat{\boldsymbol{\zeta}}_t, \mathbf{s}_{\hat{\boldsymbol{\theta}}_t} \right\rangle_{\mathcal{H}_{\mathcal{K}}^d} \leq \left\langle \mathbf{s}_{\bar{\boldsymbol{\theta}}_{t,\lambda}}, (\hat{\boldsymbol{\Gamma}}_t + \lambda \mathbf{I}) \mathbf{s}_{\bar{\boldsymbol{\theta}}_{t,\lambda}} \right\rangle_{\mathcal{H}_{\mathcal{K}}^d} + \left\langle \hat{\boldsymbol{\zeta}}_t, \mathbf{s}_{\bar{\boldsymbol{\theta}}_{t,\lambda}} \right\rangle_{\mathcal{H}_{\mathcal{K}}^d}. \quad (33)$$

Taking the derivative of $\hat{\mathcal{L}}_t(\boldsymbol{\theta}_t)$ and $\mathcal{L}_t(\boldsymbol{\theta}_t)$, we have

$$\left\langle \mathbf{s}_{\hat{\boldsymbol{\theta}}_t} - \mathbf{s}_{\bar{\boldsymbol{\theta}}_{t,\lambda}}, 2(\boldsymbol{\Gamma}_t + \lambda \mathbf{I}) \mathbf{s}_{\bar{\boldsymbol{\theta}}_{t,\lambda}} + \boldsymbol{\zeta}_t \right\rangle_{\mathcal{H}_{\mathcal{K}}^d} = 0$$

because $\hat{\boldsymbol{\theta}}_t$ and $\bar{\boldsymbol{\theta}}_{t,\lambda}$ are the minimizers of $\hat{\mathcal{L}}_t(\boldsymbol{\theta}_t)$ and $\mathcal{L}_t(\boldsymbol{\theta}_t)$, respectively. Combining this with (33), we have

$$\begin{aligned} & 2 \left\langle \mathbf{s}_{\hat{\boldsymbol{\theta}}_t} - \mathbf{s}_{\bar{\boldsymbol{\theta}}_{t,\lambda}}, (\hat{\boldsymbol{\Gamma}}_t - \boldsymbol{\Gamma}_t) \mathbf{s}_{\bar{\boldsymbol{\theta}}_{t,\lambda}} \right\rangle_{\mathcal{H}_{\mathcal{K}}^d} - \left\langle \boldsymbol{\zeta}_t, \mathbf{s}_{\hat{\boldsymbol{\theta}}_t} - \mathbf{s}_{\bar{\boldsymbol{\theta}}_{t,\lambda}} \right\rangle_{\mathcal{H}_{\mathcal{K}}^d} + \left\langle \mathbf{s}_{\hat{\boldsymbol{\theta}}_t} - \mathbf{s}_{\bar{\boldsymbol{\theta}}_{t,\lambda}}, (\hat{\boldsymbol{\Gamma}}_t + \lambda \mathbf{I}) (\mathbf{s}_{\hat{\boldsymbol{\theta}}_t} - \mathbf{s}_{\bar{\boldsymbol{\theta}}_{t,\lambda}}) \right\rangle_{\mathcal{H}_{\mathcal{K}}^d} \\ &= \left\langle \mathbf{s}_{\hat{\boldsymbol{\theta}}_t}, (\hat{\boldsymbol{\Gamma}}_t + \lambda \mathbf{I}) \mathbf{s}_{\hat{\boldsymbol{\theta}}_t} \right\rangle_{\mathcal{H}_{\mathcal{K}}^d} - \left\langle \mathbf{s}_{\bar{\boldsymbol{\theta}}_{t,\lambda}}, (\hat{\boldsymbol{\Gamma}}_t + \lambda \mathbf{I}) \mathbf{s}_{\bar{\boldsymbol{\theta}}_{t,\lambda}} \right\rangle_{\mathcal{H}_{\mathcal{K}}^d} \\ &\leq - \left\langle \hat{\boldsymbol{\zeta}}_t, \mathbf{s}_{\hat{\boldsymbol{\theta}}_t} - \mathbf{s}_{\bar{\boldsymbol{\theta}}_{t,\lambda}} \right\rangle_{\mathcal{H}_{\mathcal{K}}^d}. \end{aligned}$$

This implies that

$$\begin{aligned} & \left\langle \mathbf{s}_{\hat{\boldsymbol{\theta}}_t} - \mathbf{s}_{\bar{\boldsymbol{\theta}}_{t,\lambda}}, \boldsymbol{\Gamma}_t (\mathbf{s}_{\hat{\boldsymbol{\theta}}_t} - \mathbf{s}_{\bar{\boldsymbol{\theta}}_{t,\lambda}}) \right\rangle_{\mathcal{H}_{\mathcal{K}}^d} + \{\lambda - \delta_{2n}(\eta)\} \|\mathbf{s}_{\hat{\boldsymbol{\theta}}_t} - \mathbf{s}_{\bar{\boldsymbol{\theta}}_{t,\lambda}}\|_{\mathcal{H}_{\mathcal{K}}^d}^2 \\ &\leq \left\langle \mathbf{s}_{\hat{\boldsymbol{\theta}}_t} - \mathbf{s}_{\bar{\boldsymbol{\theta}}_{t,\lambda}}, \hat{\boldsymbol{\Gamma}}_t (\mathbf{s}_{\hat{\boldsymbol{\theta}}_t} - \mathbf{s}_{\bar{\boldsymbol{\theta}}_{t,\lambda}}) \right\rangle_{\mathcal{H}_{\mathcal{K}}^d} \\ &\leq 2 \left\langle \mathbf{s}_{\hat{\boldsymbol{\theta}}_t} - \mathbf{s}_{\bar{\boldsymbol{\theta}}_{t,\lambda}}, (\hat{\boldsymbol{\Gamma}}_t - \boldsymbol{\Gamma}_t) \mathbf{s}_{\bar{\boldsymbol{\theta}}_{t,\lambda}} \right\rangle_{\mathcal{H}_{\mathcal{K}}^d} - \left\langle \hat{\boldsymbol{\zeta}}_t - \boldsymbol{\zeta}_t, \mathbf{s}_{\hat{\boldsymbol{\theta}}_t} - \mathbf{s}_{\bar{\boldsymbol{\theta}}_{t,\lambda}} \right\rangle_{\mathcal{H}_{\mathcal{K}}^d} \\ &\leq \{\delta_{1n}(\eta) + 2\delta_{2n}(\eta)\sqrt{C_{\eta,m,\lambda}}\} \|\mathbf{s}_{\hat{\boldsymbol{\theta}}_t} - \mathbf{s}_{\bar{\boldsymbol{\theta}}_{t,\lambda}}\|_{\mathcal{H}_{\mathcal{K}}^d} \end{aligned} \quad (34)$$

according to (29), (30) and (32) with probability at least $1 - 4\eta$. Notice that

$$\left\langle \mathbf{s}_{\hat{\boldsymbol{\theta}}_t} - \mathbf{s}_{\bar{\boldsymbol{\theta}}_{t,\lambda}}, \boldsymbol{\Gamma}_t (\mathbf{s}_{\hat{\boldsymbol{\theta}}_t} - \mathbf{s}_{\bar{\boldsymbol{\theta}}_{t,\lambda}}) \right\rangle_{\mathcal{H}_{\mathcal{K}}^d} = \mathbb{E}_{\mathbf{X}_t} \left[\left\| \mathbf{s}(\mathbf{X}_t; \hat{\boldsymbol{\theta}}_t) - \mathbf{s}(\mathbf{X}_t; \bar{\boldsymbol{\theta}}_{t,\lambda}) \right\|^2 \right] \geq 0.$$

Thus,

$$\begin{aligned} \left\| \mathbf{s}_{\hat{\boldsymbol{\theta}}_t} - \mathbf{s}_{\bar{\boldsymbol{\theta}}_{t,\lambda}} \right\|_{\mathcal{H}_{\mathcal{K}}^d} &\leq \frac{\delta_{1n}(\eta) + 2\delta_{2n}(\eta)\sqrt{C_{\eta,m,\lambda}}}{\lambda - \delta_{2n}(\eta)} \\ &\leq \frac{2\{\delta_{1n}(\eta) + 2\delta_{2n}(\eta)\sqrt{C_{\eta,m,\lambda}}\}}{\lambda}. \end{aligned}$$

Then, (34) implies that

$$\mathbb{E}_{\mathbf{X}_t} \left[\left\| \mathbf{s}(\mathbf{X}_t; \hat{\boldsymbol{\theta}}_t) - \mathbf{s}(\mathbf{X}_t; \bar{\boldsymbol{\theta}}_{t,\lambda}) \right\|^2 \right] \leq \frac{2\{\delta_{1n}(\eta) + 2\delta_{2n}(\eta)\sqrt{C_{\eta,m,\lambda}}\}^2}{\lambda}.$$

Algorithm 1 Denoising with Diffusion Model

Input: Training samples $\{\mathbf{X}_1^{(i)}\}_{i=1}^n$, number of sampling steps K , tuning parameters m and λ .

- 1: **Training:**
 - 2: Obtaining parameters by closed form solution (14)
 - 3: **Sampling denoised Data:**
 - 4: **for** $i = 1, \dots, n$ **do**
 - 5: Initialized $\widehat{\mathbf{X}}_0^{(i)} = \mathbf{X}_1^{(i)}$
 - 6: **for** $k = 0, \dots, K - 1$ **do**
 - 7: Update $\widehat{\mathbf{X}}_{(k+1)/K}^{(i)}$ based on $\widehat{\mathbf{X}}_{(k+1)/K}^{(i)}$ as in (15)
 - 8: **end for**
 - 9: **end for**
 - 10: **return** Samples $\{\widehat{\mathbf{X}}_1^{(i)}\}_{i=1}^n$.
-

This together with (31) and (34) implies that

$$\begin{aligned} & \mathbb{E}_{\mathbf{X}_t} \left[\left\| \mathbf{s}(\mathbf{X}_t; \widehat{\boldsymbol{\theta}}_t) - \nabla \log p_t(\mathbf{X}_t) \right\|^2 \right] \\ & \leq \mathbb{E}_{\mathbf{X}_t} \left[\left(\left\| \mathbf{s}(\mathbf{X}_t; \bar{\boldsymbol{\theta}}_{t,\lambda}) - \nabla \log p_t(\mathbf{X}_t) \right\| + \left\| \mathbf{s}(\mathbf{X}_t; \widehat{\boldsymbol{\theta}}_t) - \mathbf{s}(\mathbf{X}_t; \bar{\boldsymbol{\theta}}_{t,\lambda}) \right\| \right)^2 \right] \\ & \leq 2\mathbb{E}_{\mathbf{X}_t} \left[\left\| \mathbf{s}(\mathbf{X}_t; \bar{\boldsymbol{\theta}}_{t,\lambda}) - \nabla \log p_t(\mathbf{X}_t) \right\|^2 \right] + 2\mathbb{E}_{\mathbf{X}_t} \left[\left\| \mathbf{s}(\mathbf{X}_t; \widehat{\boldsymbol{\theta}}_t) - \mathbf{s}(\mathbf{X}_t; \bar{\boldsymbol{\theta}}_{t,\lambda}) \right\|^2 \right] \\ & \leq 2\lambda \mathcal{B}_{\mathcal{K}} \log(\eta^{-1}) + \frac{4\sigma_0^2}{m} + 4\delta_{0m}(\eta)^2 + \frac{4\{\delta_{1n}(\eta) + 2\delta_{2n}(\eta)\sqrt{C_{\eta,m,\lambda}}\}^2}{\lambda} \end{aligned}$$

with probability at least $1 - 4\eta$, which completes the proof. \square

G Discussion on the Sampling Process

In this section, we first present the complete procedure of our diffusion-based method to tackle data with measurement error in Algorithm 1. As discussed in Section 3.3, the sampling process is numerically solving a given SDE. In fact, solving the reverse-time SDE (5) has been well explored in the existing literature related to diffusion model. One standard pipeline (Song et al., 2020b, 2022b) is transferring the target reverse SDE (2) into a distributionally equivalent Ordinary Differential

Equation (ODE) (18) by Fokker-Planck equation (Oksendal, 2013) as in Proposition 3 in Appendix. Theoretically, the samples obtained by solving the derived ODE may have smaller discretion error, compared with the ones obtained by (15), owing to the numerical priority of ODE compared to SDE (Platen, 1999).

A vast variety of literature (Bao et al., 2022; Lu et al., 2022; Xue et al., 2023; Zhao et al., 2024) improve the Euler-Maruyama method (15) by using improved numerical solver to reverse-time SDE (5) or its equivalent ODE. These improved numerical methods are quite useful in the deep learning context, since the model of score function $\mathbf{s}(\cdot; \boldsymbol{\theta}_t)$ is usually a deep neural network (LeCun et al., 2015; Ronneberger et al., 2015). Involving improved numerical methods significantly reduces the number of function evaluations (NFEs) as well as the required computational cost. However, in this paper, we use a kernel-based model $\mathbf{s}(\cdot; \boldsymbol{\theta}_t)$ to approximate the score function. Thus, the computational cost of model evaluation is not expensive, so decreasing the NFEs does not bring about significant improvement in practice.

H Ablation Study

In this section, we follow the settings in Section 5 to explore the effect of hyperparameters in our proposed method. Concretely, explore the regularization parameter λ , denoising steps K , number of samples n , and sub-samples m . Similarly, we report the MMD and MSE of varied hyperparameters. Notably, the dimension $d_{\mathbf{Z}} = 3$ and noise level $\sigma = 0.5$ across all these experiments.

The results are summarized as follows, as can be seen:

1. For regularization parameter λ in Figure 4, we find that a proper λ guarantees the best performance of our method. This is a standard phenomenon for regularization parameters (Smale and Zhou, 2003) when applying RKHS-based methods. Please notice here that the MMD is not necessary has the similar trends as MSE, since the first only depends on the quality of $\{\widehat{\mathbf{Z}}_0^{(i)}\}_{i=1}^n$, while the latter depends on that of $\{(\widehat{\mathbf{Z}}_0^{(i)}, Y_0^{(i)})\}_{i=1}^n$.
2. For denoising steps K in Figure 5, we find that increasing denoising steps does not necessarily

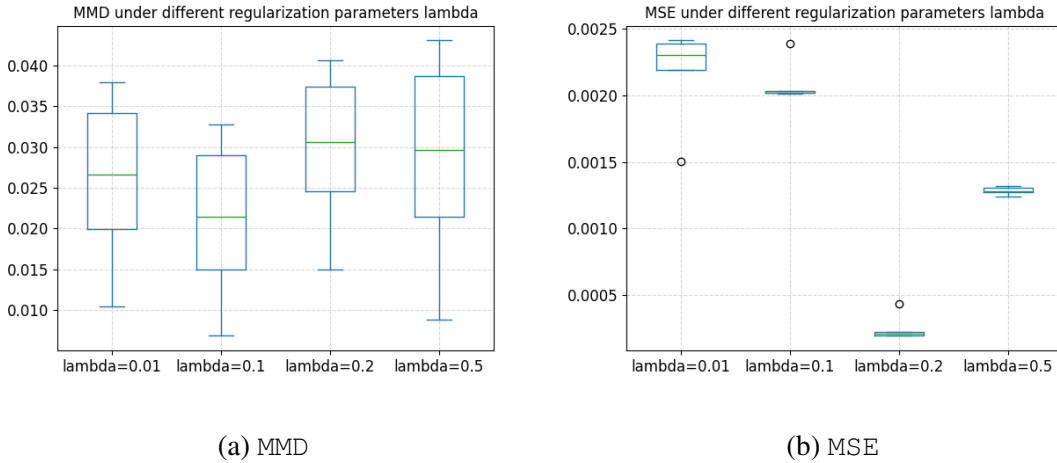


Figure 4: The MMD and MSE over different regularization parameters λ .

results in improved performance. We speculate this is because the estimation error to score function $\nabla \log p_{Z_t}(\cdot)$ is varied w.r.t. t . Thus sampling more steps on inaccurately estimated score function may induce larger error. The similar phenomenon is also observed in the diffusion model in AI (Lu et al., 2022; Bao et al., 2022; Xue et al., 2023).

3. For number of sub-samplers m in Figure 6, we find that when $m = \sqrt{n}$, the proposed algorithm has the best performance. This observation is consistent with our theoretical justification after Theorem 2.
4. For the number of samples n in Figure 7, though incrementally, we can observe that increasing the number of samples indeed improve the performance of our method, as suggested in our Theorem 2.

I Learning in Reproducing Kernel Hilbert Spaces: Some Background and Justification of Tuning Parameter Impact

Many learning problems in RKHS can be formulated as minimizing an empirical loss plus a regularization term in a *Reproducing Kernel Hilbert Space* (RKHS). Concretely, one often considers

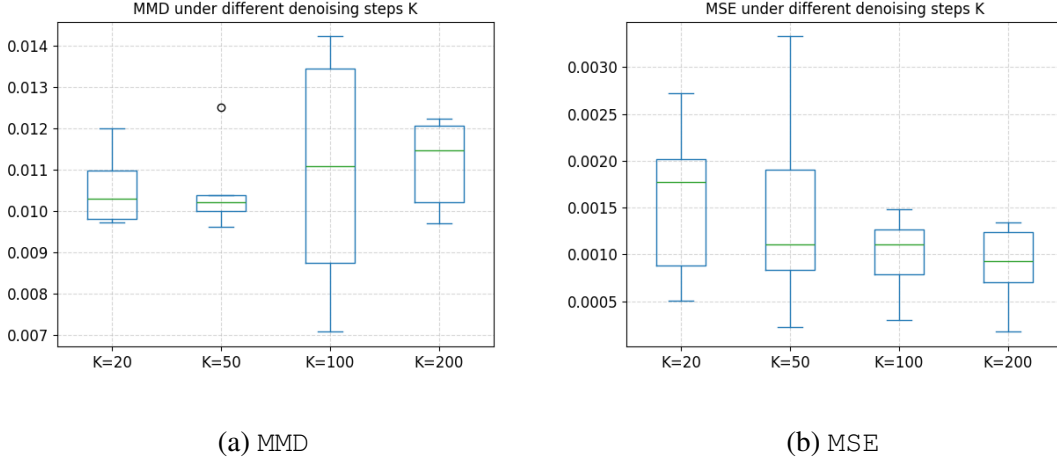


Figure 5: The MMD and MSE over different denoising steps K .

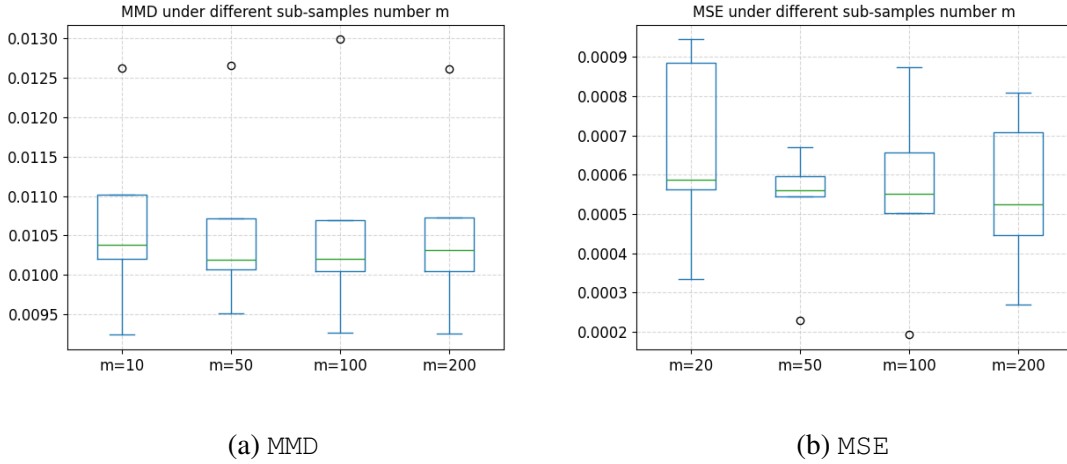


Figure 6: The MMD and MSE over different number of sub-samples m .

a problem of the form

$$\min_{f \in \mathcal{H}_{\mathcal{K}}} \left\{ \frac{1}{n} \sum_{i=1}^n \left(Y^{(i)} - f(\mathbf{X}^{(i)}) \right)^2 + \lambda \|f\|_{\mathcal{H}_{\mathcal{K}}}^2 \right\}, \quad (35)$$

where $\mathcal{H}_{\mathcal{K}}$ is a RKHS with reproducing kernel $\mathcal{K}(\cdot, \cdot)$, $\{(\mathbf{X}^{(i)}, y^i)\}_{i=1}^n$ are training data, and $\lambda > 0$ is the regularization parameter. In this paper, we conduct such regression for each dimension of the target score function, i.e., the $\mathbf{X}^{(i)}$ is supposed to be $\mathbf{X}_t^{(i)}$ and $Y^{(i)}$ is one specific dimension of $\nabla \log p_t(\mathbf{X}_t^{(i)})$, where $\mathbf{X}_t^{(i)} \sim P_{\mathbf{X}_t}$. Though these data are unobservable, we fix this issue by our method in Section 3.

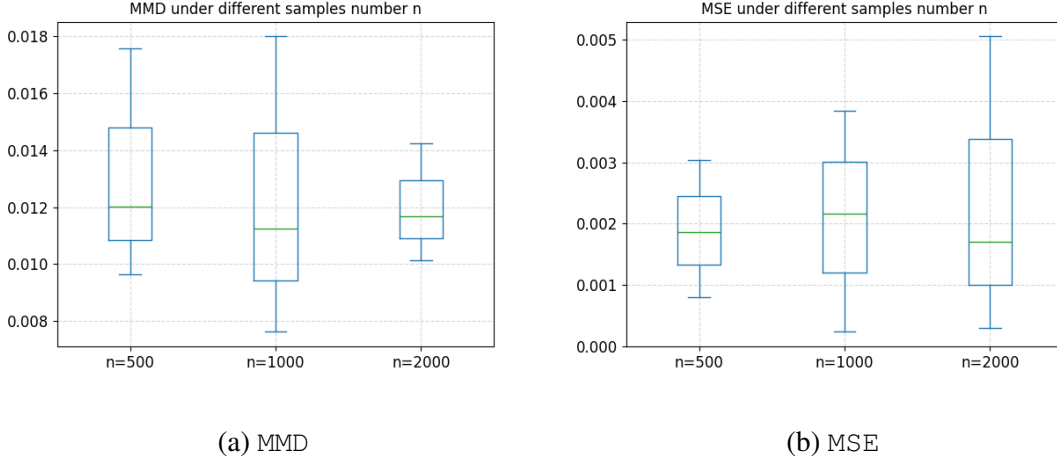


Figure 7: The MMD and MSE over different number of samples n .

By representation theorem, the minimizer $f(\cdot)$ of (35) takes the form

$$f(\mathbf{x}) = \sum_{i=1}^n \alpha_i \mathcal{K}(\mathbf{x}, \mathbf{X}^{(i)}),$$

where $\boldsymbol{\alpha} = (\alpha_1, \dots, \alpha_n)$ satisfying.

$$\boldsymbol{\alpha} = (\mathbf{K} + \lambda \mathbf{I})^{-1} \mathbf{K} \mathbf{Y},$$

where \mathbf{K} is a $n \times n$ matrix with its i, j -th element is $\mathcal{K}(\mathbf{X}^{(i)}, \mathbf{X}^{(j)})$, $\mathbf{Y} = (Y^{(1)}, \dots, Y^{(n)})$. As can be seen here, the regularization parameter λ here makes the matrix $\mathbf{K} + \lambda \mathbf{I}$ invertible, while increasing it will make the obtained f away from the ground-truth target. Notably, such a gap has an explicit dependence on λ , which usually depends on the smoothness of the target function i.e., $\nabla \log p_t(\cdot)$ in this paper (Smale and Zhou, 2003; De Vito et al., 2005). Assumption 4 implies that the target score can be approximated well by (infinitely smooth) analytic functions, thus we can derive a sharp approximation error by selecting $\lambda = \mathcal{O}(n^{-1/2})$ as in Section 4.2.

In this paper, we set the kernel function $\mathcal{K}(\cdot, \cdot)$ as the Gaussian kernel

$$\mathcal{K}(\mathbf{x}_1, \mathbf{x}_2) = \exp \left\{ -(\mathbf{x}_1 - \bar{\mathbf{x}}_2)^\top \mathbf{H} (\mathbf{x}_1 - \bar{\mathbf{x}}_2) \right\},$$

in complex ordinate space. As suggested above, instead of optimizing over infinitely many possible functions in $\mathcal{H}_{\mathcal{K}}$, one only needs to solve for finite coefficients, as we did in Section 3.2 by restricting

$s_{tl}(\cdot, \boldsymbol{\theta}_t) \in \mathcal{H}_{\mathcal{K}_t, m}^d$. The Gaussian kernel is an analytic function, and a universal approximator. Proposition 1 shows that functions in $\mathcal{H}_{\mathcal{K}_t, m}$ can approximate the target score function $\nabla \log p_t(\cdot)$ well.

Notably, for the model based in RKHS (De Vito et al., 2005; Smale and Zhou, 2003, 2007), we do not select the \mathbf{H} i.e., bandwidth, as in classical kernel density estimation, where their bandwidth depends on data dimension. To make such a selection, we should explicitly compute the dependence of $\mathcal{B}_{\mathcal{K}}$ on \mathbf{H} , which is hard and we leave it for future work.

J MMD Distance

The Maximum Mean Discrepancy (MMD) distance measures the difference between two probability distributions with the same support. For such MMD between distributions P, Q , it is defined as

$$\text{MMD}(P, Q) = \sup_{f \in \mathcal{H}_{\mathcal{K}}} |\mathbb{E}_P[f] - \mathbb{E}_Q[f]|,$$

where $\mathcal{H}_{\mathcal{K}}$ is the RKHS induced by positive semi-definite kernel $\mathcal{K}(\cdot, \cdot)$. Notably, the above equation has an equivalent formulation such that

$$\text{MMD}(P, Q) = \mathbb{E}_{P \times P}[\mathcal{K}(\mathbf{X}, \mathbf{Y})] - 2\mathbb{E}_{P \times Q}[\mathcal{K}(\mathbf{X}, \mathbf{Y})] + \mathbb{E}_{Q \times Q}[\mathcal{K}(\mathbf{X}, \mathbf{Y})].$$

With this in hand, we can directly estimate the MMD by its empirical version without requiring the explicit formulation of distributions P, Q . Thus, we select such metric in Section 5. Our used kernel is a composition of five Gaussian kernels with different bandwidths as in (Li et al., 2015).

K Additional Figures in the Diabetes Clinical Case Study

The variations in glucose time-in-range metrics for control and treatment groups at different noise levels are in Figure 8.

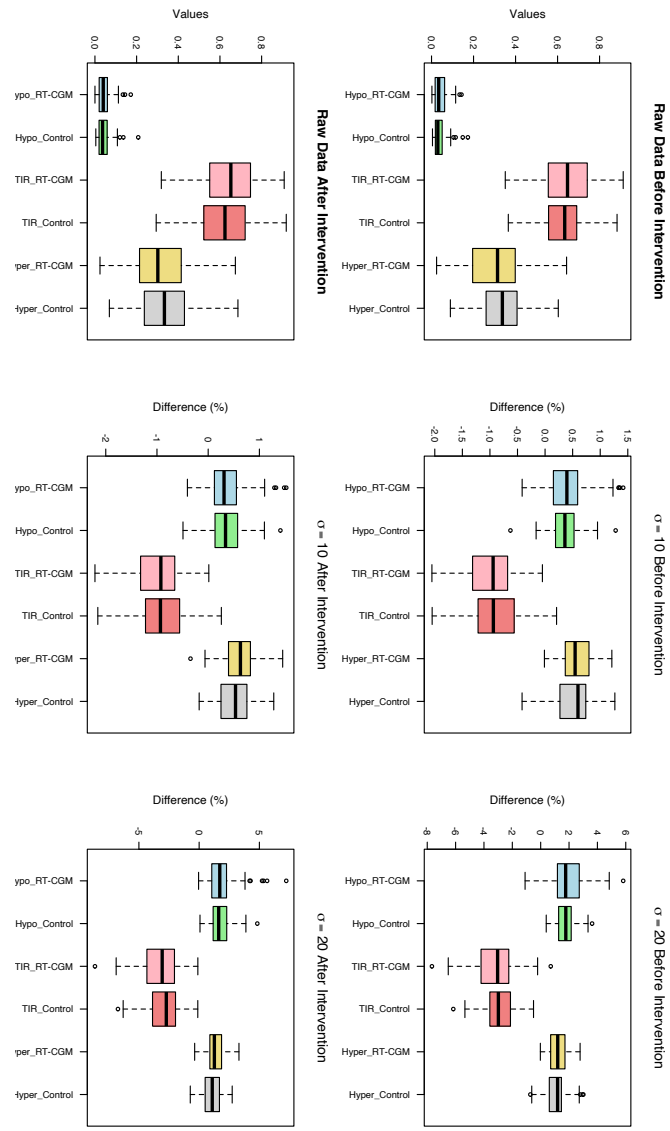


Figure 8: Variations in glucose time-in-range metrics for control and treatment groups at noise levels $\sigma = 0, 10, 20$ before and after interventions.

References

- Anderson, B. D. (1982), “Reverse-time diffusion equation models,” *Stochastic Processes and their Applications*, 12, 313–326.
- Bao, F., Li, C., Zhu, J., and Zhang, B. (2022), “Analytic-DPM: an Analytic Estimate of the Optimal Reverse Variance in Diffusion Probabilistic Models,” in *International Conference on Learning Representations*.
- Bauer, F., Pereverzev, S., and Rosasco, L. (2007), “On regularization algorithms in learning theory,” *Journal of Complexity*, 23, 52–72.
- Belomestny, D. and Goldenshluger, A. (2021), “Density deconvolution under general assumptions on the distribution of measurement errors,” *The Annals of Statistics*, 49, 615–649.
- Bent, B., Goldstein, B. A., Kibbe, W. A., and Dunn, J. P. (2020), “Investigating sources of inaccuracy in wearable optical heart rate sensors,” *NPJ digital medicine*, 3, 18.
- Bovy, J., Hogg, D. W., and Roweis, S. T. (2011), “Extreme deconvolution: Inferring complete distribution functions from noisy, heterogeneous and incomplete observations,” *The Annals of Applied Statistics*, 1657–1677.
- Brodley, C. E. and Friedl, M. A. (1999), “Identifying mislabeled training data,” *Journal of Artificial Intelligence Research*, 11, 131–167.
- Carroll, R. J. and Hall, P. (1988), “Optimal rates of convergence for deconvolving a density,” *Journal of the American Statistical Association*, 83, 1184–1186.
- Carroll, R. J., Küchenhoff, H., Lombard, F., and Stefanski, L. A. (1996), “Asymptotics for the SIMEX estimator in nonlinear measurement error models,” *Journal of the American Statistical Association*, 91, 242–250.

- Carroll, R. J., Ruppert, D., Stefanski, L. A., and Crainiceanu, C. M. (2006), *Measurement Error in Nonlinear Models: A Modern Perspective*, Chapman and Hall/CRC.
- Chen, S., Chewi, S., Lee, H., Li, Y., Lu, J., and Salim, A. (2023), “The probability flow ODE is provably fast,” Preprint arXiv:2305.11798.
- Chen, S., Chewi, S., Li, J., Li, Y., Salim, A., and Zhang, A. (2022), “Sampling is as easy as learning the score: theory for diffusion models with minimal data assumptions,” in *International Conference on Learning Representations*.
- Chen, Z., Yi, G. Y., and Wu, C. (2011), “Marginal methods for correlated binary data with misclassified responses,” *Biometrika*, 98, 647–662.
- Chewi, S. (2023), “Log-concave sampling,” *Lecture Notes*.
- Cordy, C. B. and Thomas, D. R. (1997), “Deconvolution of a distribution function,” *Journal of the American Statistical Association*, 92, 1459–1465.
- Cover, T. M. (1999), *Elements of Information Theory*, John Wiley & Sons.
- Daras, G., Shah, K., Dagan, Y., Gollakota, A., Dimakis, A., and Klivans, A. (2024), “Ambient diffusion: Learning clean distributions from corrupted data,” *Advances in Neural Information Processing Systems*.
- De Vito, E., Rosasco, L., Caponnetto, A., De Giovannini, U., Odone, F., and Bartlett, P. (2005), “Learning from Examples as an Inverse Problem.” *Journal of Machine Learning Research*, 6, 883–904.
- Delaigle, A. and Hall, P. (2008), “Using SIMEX for smoothing-parameter choice in errors-in-variables problems,” *Journal of the American Statistical Association*, 103, 280–287.
- Desiere, S. and Jolliffe, D. (2018), “Land productivity and plot size: Is measurement error driving the inverse relationship?” *Journal of Development Economics*, 130, 84–98.

- Efron, B. (2011), “Tweedie’s formula and selection bias,” *Journal of the American Statistical Association*, 106, 1602–1614.
- Fan, J. (1991), “On the Optimal Rates of Convergence for Nonparametric Deconvolution Problems,” *The Annals of Statistics*, 19, 1257–1272.
- Frisch, R. (1934), “Statistical confluence analysis by means of complete regression systems,” .
- Garg, S., Ramakrishnan, G., and Thumbe, V. (2021), “Towards robustness to label noise in text classification via noise modeling,” in *ACM International Conference on Information & Knowledge Management*.
- Guan, Z. (2021), “Fast nonparametric maximum likelihood density deconvolution using Bernstein polynomials,” *Statistica Sinica*, 31, 891–908.
- Hall, P. and Maiti, T. (2009), “Deconvolution methods for non-parametric inference in two-level mixed models,” *Journal of the Royal Statistical Society Series B: Statistical Methodology*, 71, 703–718.
- Havrilla, A. and Iyer, M. (2024), “Understanding the Effect of Noise in LLM Training Data with Algorithmic Chains of Thought,” Preprint arXiv:2402.04004.
- He, K., Zhang, X., Ren, S., and Sun, J. (2015), “Delving deep into rectifiers: Surpassing human-level performance on imagenet classification,” in *International Conference on Computer Vision*.
- Ho, J., Jain, A., and Abbeel, P. (2020), “Denoising diffusion probabilistic models,” in *Advances in Neural Information Processing Systems*.
- Hofmann, T., Schölkopf, B., and Smola, A. J. (2008), “Kernel methods in machine learning,” .
- Hyvärinen, A. and Dayan, P. (2005), “Estimation of non-normalized statistical models by score matching.” *Journal of Machine Learning Research*, 6, 695–709.

- JDRF CGM Study Group (2009), “The effect of continuous glucose monitoring in well-controlled type 1 diabetes,” *Diabetes Care*, 32, 1378–1383.
- Jiang, F., Zhou, Y., Liu, J., and Ma, Y. (2023), “On high-dimensional Poisson models with measurement error: Hypothesis testing for nonlinear nonconvex optimization,” *The Annals of Statistics*, 51, 233–259.
- Jiang, Z. and Ding, P. (2020), “Measurement errors in the binary instrumental variable model,” *Biometrika*, 107, 238–245.
- Kawar, B., Elata, N., Michaeli, T., and Elad, M. (2023), “Gsurre-based diffusion model training with corrupted data,” Preprint arXiv:2305.13128.
- Kim, J. and Scott, C. D. (2012), “Robust kernel density estimation,” *The Journal of Machine Learning Research*, 13, 2529–2565.
- Kingma, D. P. and Welling, M. (2013), “Auto-encoding variational Bayes,” in *International Conference on Learning Representations*.
- Lachin, J. M. (2004), “The role of measurement reliability in clinical trials,” *Clinical Trials*, 1, 553–566, PMID: 16279296.
- LeCun, Y., Bengio, Y., and Hinton, G. (2015), “Deep learning,” *Nature*, 521, 436–444.
- Lee, H., Lu, J., and Tan, Y. (2022), “Convergence for score-based generative modeling with polynomial complexity,” in *Advances in Neural Information Processing Systems*.
- Lepski, O. and Willer, T. (2019), “Oracle inequalities and adaptive estimation in the convolution structure density model,” *The Annals of Statistics*, 47, 233–287.
- Li, G., Wei, Y., Chen, Y., and Chi, Y. (2024), “Towards non-asymptotic convergence for diffusion-based generative models,” in *International Conference on Learning Representations*.

- Li, J., Xiong, C., and Hoi, S. C. (2021), “Learning from noisy data with robust representation learning,” in *International Conference on Computer Vision*.
- Li, X., Thackstun, J., Gulrajani, I., Liang, P. S., and Hashimoto, T. B. (2022), “Diffusion-lm improves controllable text generation,” in *Advances in Neural Information Processing Systems*.
- Li, Y., Swersky, K., and Zemel, R. (2015), “Generative moment matching networks,” in *International Conference on Machine Learning*.
- Lin, Z., Gong, Y., Shen, Y., Wu, T., Fan, Z., Lin, C., Duan, N., and Chen, W. (2023), “Text generation with diffusion language models: A pre-training approach with continuous paragraph denoise,” in *International Conference on Machine Learning*.
- Liu, X., Gong, C., and Liu, Q. (2022), “Flow straight and fast: Learning to generate and transfer data with rectified flow,” Preprint arXiv:2209.03003.
- Loh, P.-L. and Wainwright, M. J. (2012), “HIGH-DIMENSIONAL REGRESSION WITH NOISY AND MISSING DATA: PROVABLE GUARANTEES WITH NONCONVEXITY,” *The Annals of Statistics*, 40, 1637–1664.
- Loken, E. and Gelman, A. (2017), “Measurement error and the replication crisis,” *Science*, 355, 584–585.
- Lounici, K. and Nickl, R. (2011), “Global uniform risk bounds for wavelet deconvolution estimators,” *The Annals of Statistics*, 39, 201–231.
- Lu, C., Zhou, Y., Bao, F., Chen, J., Li, C., and Zhu, J. (2022), “DPM-Solver: A Fast ODE Solver for Diffusion Probabilistic Model Sampling in Around 10 Steps,” in *Advances in Neural Information Processing Systems*.
- Ma, X., Wang, Y., Jia, G., Chen, X., Liu, Z., Li, Y.-F., Chen, C., and Qiao, Y. (2024), “Latte: Latent diffusion transformer for video generation,” Preprint arXiv:2401.03048.

- Madry, A., Makelov, A., Schmidt, L., Tsipras, D., and Vladu, A. (2017), “Towards deep learning models resistant to adversarial attacks,” Preprint arXiv:1706.06083.
- Masry, E. (1993), “Strong consistency and rates for deconvolution of multivariate densities of stationary processes,” *Stochastic Processes and Their Applications*, 47, 53–74.
- Matabuena, M., Felix, P., Garcia-Meixide, C., and Gude, F. (2022), “Kernel machine learning methods to handle missing responses with complex predictors. Application in modelling five-year glucose changes using distributional representations,” *Computer Methods and Programs in Biomedicine*, 221, 106905.
- Matabuena, M., Ghosal, R., Aguilar, J. E., Wagner, R., Merino, C. F., Castro, J. S., Zipunnikov, V., Onnela, J.-P., and Gude, F. (2024a), “Glucodensity Functional Profiles Outperform Traditional Continuous Glucose Monitoring Metrics,” Preprint arXiv:2410.00912.
- Matabuena, M., Ghosal, R., Mozharovskiy, P., Padilla, O. H. M., and Onnela, J.-P. (2024b), “Conformal uncertainty quantification using kernel depth measures in separable Hilbert spaces,” *arXiv preprint arXiv:2405.13970*.
- Matabuena, M., Petersen, A., Vidal, J. C., and Gude, F. (2021), “Glucodensities: A new representation of glucose profiles using distributional data analysis,” *Statistical Methods in Medical Research*, 30, 1445–1464, PMID: 33760665.
- Meister, A. and Neumann, M. H. (2010), “Deconvolution from non-standard error densities under replicated measurements,” *Statistica Sinica*, 1609–1636.
- Muandet, K., Fukumizu, K., Sriperumbudur, B., Schölkopf, B., et al. (2017), “Kernel mean embedding of distributions: A review and beyond,” *Foundations and Trends® in Machine Learning*, 10, 1–141.
- Nakamura, T. (1990), “Corrected score function for errors-in-variables models: Methodology and application to generalized linear models,” *Biometrika*, 77, 127–137.

- Oksendal, B. (2013), *Stochastic Differential Equations: An Introduction with Applications*, Springer Science & Business Media.
- Peebles, W. and Xie, S. (2023), “Scalable diffusion models with transformers,” in *International Conference on Computer Vision*.
- Platen, E. (1999), “An introduction to numerical methods for stochastic differential equations,” *Acta Numerica*, 8, 197–246.
- Prentice, R. L. (1982), “Covariate measurement errors and parameter estimation in a failure time regression model,” *Biometrika*, 69, 331–342.
- Robbins, H. and Monro, S. (1951), “A stochastic approximation method,” *The Annals of Mathematical Statistics*, 400–407.
- Rombach, R., Blattmann, A., Lorenz, D., Esser, P., and Ommer, B. (2022), “High-resolution image synthesis with latent diffusion models,” in *Conference on Computer Vision and Pattern Recognition*.
- Ronneberger, O., Fischer, P., and Brox, T. (2015), “U-net: Convolutional networks for biomedical image segmentation,” in *Medical Image Computing and Computer-Assisted Intervention*.
- Sarkar, A., Pati, D., Chakraborty, A., Mallick, B. K., and Carroll, R. J. (2018), “Bayesian semiparametric multivariate density deconvolution,” *Journal of the American Statistical Association*, 113, 401–416.
- Schennach, S. M. (2016), “Recent Advances in the Measurement Error Literature,” *Annual Review of Economics*, 8, 341–377.
- Schuster, I., Mollenhauer, M., Klus, S., and Muandet, K. (2020), “Kernel conditional density operators,” in *International Conference on Artificial Intelligence and Statistics*.

- Smale, S. and Zhou, D.-X. (2003), “Estimating the approximation error in learning theory,” *Analysis and Applications*, 1, 17–41.
- (2007), “Learning theory estimates via integral operators and their approximations,” *Constructive Approximation*, 26, 153–172.
- Sohl-Dickstein, J., Weiss, E., Maheswaranathan, N., and Ganguli, S. (2015), “Deep unsupervised learning using nonequilibrium thermodynamics,” in *International Conference on Machine Learning*.
- Song, H., Kim, M., Park, D., Shin, Y., and Lee, J.-G. (2022a), “Learning from noisy labels with deep neural networks: A survey,” *IEEE Transactions on Neural Networks and Learning Systems*, 34, 8135–8153.
- Song, J., Meng, C., and Ermon, S. (2022b), “Denoising Diffusion Implicit Models,” in *International Conference on Learning Representations*.
- Song, Y., Durkan, C., Murray, I., and Ermon, S. (2021), “Maximum likelihood training of score-based diffusion models,” in *Advances in Neural Information Processing Systems*.
- Song, Y., Garg, S., Shi, J., and Ermon, S. (2020a), “Sliced score matching: A scalable approach to density and score estimation,” in *Uncertainty in Artificial Intelligence*.
- Song, Y., Sohl-Dickstein, J., Kingma, D. P., Kumar, A., Ermon, S., and Poole, B. (2020b), “Score-Based Generative Modeling through Stochastic Differential Equations,” in *International Conference on Learning Representations*.
- Sriperumbudur, B., Fukumizu, K., Gretton, A., Hyv, A., Kumar, R., et al. (2017), “Density estimation in infinite dimensional exponential families,” *Journal of Machine Learning Research*, 18, 1–59.
- Stefanski, L. A. and Carroll, R. J. (1987), “Conditional scores and optimal scores for generalized linear measurement-error models,” *Biometrika*, 74, 703–716.

- Stefanski, L. A. and Cook, J. R. (1995), “Simulation-extrapolation: the measurement error jackknife,” *Journal of the American Statistical Association*, 90, 1247–1256.
- Tamborlane, W., Beck, R., Bode, B., et al. (2008), “Continuous Glucose Monitoring and Intensive Treatment of Type 1 Diabetes,” *New England Journal of Medicine*, 359, 1464–1476.
- Thompson, J. R. and Carter, R. L. (2007), “An overview of normal theory structural measurement error models,” *International Statistical Review*, 75, 183–198.
- Van der Vaart, A. W. (2000), *Asymptotic Statistics*, vol. 3, Cambridge university press.
- Vincent, P. (2011), “A connection between score matching and denoising autoencoders,” *Neural Computation*, 23, 1661–1674.
- Wahba, G. (1990), *Spline Models for Observational Data*, SIAM.
- Wainwright, M. J. (2019), *High-Dimensional Statistics: A Non-asymptotic Viewpoint*, vol. 48, Cambridge University Press.
- Wang, C.-Y. and Sullivan Pepe, M. (2000), “Expected estimating equations to accommodate covariate measurement error,” *Journal of the Royal Statistical Society Series B: Statistical Methodology*, 62, 509–524.
- Wang, H. J., Stefanski, L. A., and Zhu, Z. (2012), “Corrected-loss estimation for quantile regression with covariate measurement errors,” *Biometrika*, 99, 405–421.
- Wang, R., Yi, M., Chen, Z., and Zhu, S. (2022), “Out-of-distribution generalization with causal invariant transformations,” in *Conference on Computer Vision and Pattern Recognition*.
- Wang, X.-F. and Wang, B. (2011), “Deconvolution estimation in measurement error models: the R package decon,” *Journal of Statistical Software*, 39.
- Wasserman, L. (2006), *All of Nonparametric Statistics*, Springer Science & Business Media.

- Welling, M. and Teh, Y. W. (2011), “Bayesian learning via stochastic gradient Langevin dynamics,” in *International Conference on Machine Learning*.
- Xiao, T., Xia, T., Yang, Y., Huang, C., and Wang, X. (2015), “Learning from massive noisy labeled data for image classification,” in *Conference on Computer Vision and Pattern Recognition*.
- Xue, S., Yi, M., Luo, W., Zhang, S., Sun, J., Li, Z., and Ma, Z.-M. (2023), “SA-Solver: Stochastic Adams Solver for Fast Sampling of Diffusion Models,” in *Advances in Neural Information Processing Systems*.
- Yan, Y. and Yi, G. Y. (2015), “A corrected profile likelihood method for survival data with covariate measurement error under the Cox model,” *Canadian Journal of Statistics*, 43, 454–480.
- Yang, Y., Pilanci, M., and Wainwright, M. J. (2017), “Randomized sketches for kernels: fast and optimal nonparametric regression,” *The Annals of Statistics*, 45, 991–1023.
- Yi, G. (2017), “Statistical Analysis with Measurement Error or Misclassification: Strategy, Method and Application,” *Springer Series in Statistics*, 1–479.
- Yi, M., Hou, L., Sun, J., Shang, L., Jiang, X., Liu, Q., and Ma, Z. (2021), “Improved ood generalization via adversarial training and pretraing,” in *International Conference on Machine Learning*.
- Yi, M., Li, A., Xin, Y., and Li, Z. (2024), “Towards Understanding the Working Mechanism of Text-to-Image Diffusion Model,” in *Advances in Neural Information Processing Systems*.
- Yi, M., Sun, J., and Li, Z. (2023a), “On the generalization of diffusion model,” Preprint arXiv:2305.14712.
- Yi, M., Wang, R., Sun, J., Li, Z., and Ma, Z.-M. (2023b), “Breaking Correlation Shift via Conditional Invariant Regularizer,” in *The International Conference on Learning Representations*.

- Zhang, C.-H. (1990), “Fourier methods for estimating mixing densities and distributions,” *The Annals of Statistics*, 806–831.
- Zhang, J., Xue, F., Xu, Q., Lee, J., and Qu, A. (2024), “Individualized dynamic latent factor model for multi-resolutional data with application to mobile health,” *Biometrika*, asae015.
- Zhang, Y., Duchi, J., and Wainwright, M. (2015), “Divide and conquer kernel ridge regression: A distributed algorithm with minimax optimal rates,” *The Journal of Machine Learning Research*, 16, 3299–3340.
- Zhao, W., Bai, L., Rao, Y., Zhou, J., and Lu, J. (2024), “Unipc: A unified predictor-corrector framework for fast sampling of diffusion models,” in *Advances in Neural Information Processing Systems*.
- Zheng, Z., Peng, X., Yang, T., Shen, C., Li, S., Liu, H., Zhou, Y., Li, T., and You, Y. (2024), “Open-Sora: Democratizing Efficient Video Production for All,” .
- Zhou, Y., Shi, J., and Zhu, J. (2020), “Nonparametric score estimators,” in *International Conference on Machine Learning*.
- Zucker, D. M. (2005), “A pseudo-partial likelihood method for semiparametric survival regression with covariate errors,” *Journal of the American Statistical Association*, 100, 1264–1277.